Thermal evolution of planetesimals during accretion

Y. Ricard[a], D. Bercovici[b], F. Albarède[a]

[a]Université de Lyon, Ens de Lyon, CNRS, Université Lyon 1, Laboratoire de Sciences de la Terre, 15 parvis René Descartes, 69007, France.

[b]Department of Geology & Geophysics, Yale University, PO Box 208109, New Haven, Connecticut, 06520-8109, USA

Abstract

Although the mass distribution of planetesimals during the early stages of planetary formation has been discussed in various studies, this is not the case for their temperature distribution. Mass and temperature distributions are closely linked, since the ability of planetesimals to dissipate the heat produced by both radioactive decay and impacts is related to their size and hence mass. Here, we propose a simple model of the evolution of the joint mass-temperature distribution through a formalism that encompasses the classic statistical approach of Wetherill (1990). We compute the statistical distribution of planetesimals by using simple rules for aggregation. Although melting temperatures can be easily reached, the formation of molten planetary embryos requires that they be formed in only a few 100 kyr. Our aggregation model, which even ignores fragmentation during collision, predicts that planetesimals with radii less than approximately 20 km will not melt during their formation.

Keywords: Planetesimals, Planetary formation, Thermal histories, Accretion, Asteroid vesta

1. Introduction

During the earlier stages of planetary accretion, the mass distribution of planetesimals evolved through collisions (i.e., merging of planetesimals). This process of planetary accretion has been initially described analytically with conceptual and statistical models (Wetherill & Stewart, 1989; Wetherill, 1990) and then including a more realistic physics (e.g., Kenyon & Luu, 1998). Recently the dramatic increase in computer capabilities has allowed the researchers to simulate the accretion with N-body simulations. However, models that end up with a planetary system somewhat akin to ours are still based on assumptions that are not fully justified and are sometimes contradictory such as a specific density profile in the nebula (Izidoro et al., 2014), a complex radial drift of the giant planets (the grand tack model of Walsh et al. (2011)) or a specific production of small scale planetesimals (the pebble model of Lambrechts & Johansen (2012) and Levison et al. (2015)). For obvious computational limitations, the N-body codes can only deal with a large but limited number of gravitating objects and a limited number of simulations and therefore does not efficiently explore the field of possible solutions. The exact distribution of planetesimal sizes as a function of time and distance to the sun is still poorly known.

Although the distribution of planetesimal sizes has been addressed, this is not the case for their thermal evolution and distribution in temperatures. In between collisions, the internal temperature of the planetesimals varied by radioactive heat release, mostly the decay of ^{26}Al, (Lee et al., 1976) and radiative heat loss at their surface. Collisions were also accompanied by a partial release of the impactor's kinetic energy into the target planetesimal (Tonks & Melosh, 1993;

Monteux et al., 2009). Gravitational energy release during planetesimal differentiation was a last source of thermal energy (Birch, 1965; Flasar & Birch, 1973; Ricard et al., 2009). Dissipation of impact energy and gravitational heat release, related to gravity, required an already large mass for the planetesimal.

Various studies have produced models of accretion for a planetesimal by imposing a given history of formation (e.g., Senshu et al., 2002; Yoshino et al., 2003; Merk & Prialnik, 2003; Walter & Tronnes, 2004; Merk & Prialnik, 2006; Sramek et al., 2012). However, as the resulting temperatures are strong functions of the accretion history (Merk et al., 2002; Sramek et al., 2012), a statistical evaluation of the joint distribution of temperatures and sizes is needed and is therefore presented in the rest of this paper. For this novel attempt, it would be a formidable task to couple the most sophisticated N-body models of planetary accretion to a precise model of temperature evolution inside each planetesimal. We therefore use the classic and versatile statistical approach of Wetherill (1990) for accretion and put our effort onto the thermal evolution of the planetesimals.

2. Statistical distribution of masses and temperatures

2.1. Mass distribution evolution during coalescence

There are various domains of science where large bodies are produced by a discontinuous coalescence of smaller units. Such processes occur in chemistry (e.g., in polymer production; Stockmayer, 1943), in aerosol formation and growth (e.g., Gelbard & Seinfeld, 1979; Pilinis, 1990), in life science (e.g., during cellular or population growth; Neelamegham et al., 1997; Ackleh & Fitzpatrick, 1997) and is central to planetary accretion (Wetherill & Stewart, 1989; Wetherill, 1990; Inaba et al., 1999, 2001). The reverse process occurs in the case of forming small bodies by fragmentation of a larger one (Wetherill & Stewart, 1993; Collet, 2004). In a very general approach, the number of bodies $\mathrm{d}N$ with masses between $m - \mathrm{d}m/2$ and $m + \mathrm{d}m/2$ (or with size R, between $R - \mathrm{d}R/2$ and $R + \mathrm{d}R/2$, although using a conserved quantity like mass is more convenient) is defined by a distribution function $\mathcal{V}(t, m)$ in kg^{-1} (i.e., in number of planetesimals in a mass interval of 1 kg)

$$\mathrm{d}N = \mathcal{V}\mathrm{d}m. \tag{1}$$

This mass distribution evolves with time according to

$$\frac{\mathrm{d}\mathcal{V}}{\mathrm{d}t} = \Gamma \tag{2}$$

where $\Gamma(t, m, \mathcal{V})$ (in kg^{-1}s^{-1}) is the rate of formation of bodies of size m at time t; Γ must also satisfy mass conservation and is therefore a function of the distribution $\mathcal{V}(t, m)$ itself. In equation (2), we use a d/dt for the time derivative instead of a $\partial/\partial t$ to remind that the distribution can also be advected by a velocity field. Analysis of the evolution of size distribution has long history starting from von Smoluchowski (1917) (see reviews from Collet & Goudon (2000); Collet (2004); Leyvraz (2005)).

2.2. Mass distribution evolution by continuous process

Contrary to the "discontinuous" processes of coalescence/fragmentation that change the number of objects that are interacting, "continuous" processes can modify the mass distribution of a collection of objects without changing their number. For exemple, in material sciences, the size distribution of solid grains solidifying from a melt and their coarsening through time has been the subject of research for many decades (e.g., Lifshitz & Slyozov, 1961; Hillert, 1965). The population of grains of a given mass evolves continuously by mass diffusion with grains belonging to immediate neighboring populations (i.e., the population of masses in the range $[m-\mathrm{d}m/2, m+\mathrm{d}m/2]$ gets or loses mass from populations in the ranges $[m-3\mathrm{d}m/2, m-\mathrm{d}m/2]$ and $[m+\mathrm{d}m/2, m+3\mathrm{d}m/2]$). This process has been described by the equation

$$\frac{\mathrm{d}\mathcal{V}}{\mathrm{d}t}+\frac{\partial \dot{m}\mathcal{V}}{\partial m}=0, \tag{3}$$

where $\dot{m}$ is the rate of change of mass for a given coarsening grain (Lifshitz & Slyozov, 1961; Hillert, 1965). Notice that equation (3) is the four-dimensional generalization of the usual conservation equation in three dimensions; to wit, in the space (x, y, z, m), the velocity is $v_4 = (v_x, v_y, v_z, \dot{m})$, the gradient operator is $\nabla_4 = (\partial/\partial x, \partial/\partial y, \partial/\partial z, \partial/\partial m)$ and the distribution obeys $\partial\mathcal{V}/\partial t+\nabla_4(v_4\mathcal{V}) = 0$. This 4-D formalism used in Ricard & Bercovici (2009) could be extended to account for other continuous variables (see e.g., Randolph & Larson, 1988).

2.3. *General mass distribution evolution*

Of course, both continuous and discontinuous processes can occur simultaneously, controlled by an equation of the general form

$$\frac{\mathrm{d}\mathcal{V}}{\mathrm{d}t}+\frac{\partial \dot{m}\mathcal{V}}{\partial m}=\Gamma. \tag{4}$$

We proposed a model for the grain size evolution of planetary mantle material based on this equation where grain coarsening occurs continuously but where grain comminution (recrystallization, fragmentation) occurs discontinuously (Ricard & Bercovici, 2009). This approach has been shown to be in agreement with experiments (Rozel et al., 2011) and when coupled with a rheological model and extended into two-phases to allow interaction between immiscible components, i.e. through Zener pinning, can be used to help explain the occurrence on plate tectonics on Earth (Bercovici & Ricard, 2012, 2013, 2014).

2.4. *Mass and thermal energy distribution of planetesimals*

We now add the thermal energy as a new variable and identify a planetesimal in mass and energy space with the notation "(m, ε)", which in fact represents a planetesimal with mass and thermal energy in the ranges $[m-\mathrm{d}m/2, m+\mathrm{d}m/2]$ and $[\varepsilon-\mathrm{d}\varepsilon/2, \varepsilon+\mathrm{d}\varepsilon/2]$. There are $\mathrm{d}n(t, m, \varepsilon)$ such planetesimals so that

$$\mathrm{d}n = \mathcal{W}\,\mathrm{d}m\mathrm{d}\varepsilon \tag{5}$$

where $\mathcal{W}(t, m, \varepsilon)$ (in $\mathrm{kg}^{-1}\mathrm{J}^{-1}$) is the mass and energy distribution of planetesimals.

The histogram of planetesimal properties $\mathcal{W}(t, m, \varepsilon)$ evolves by merging and breaking planetesimals. It also evolves by radioactive heat production, dissipation, heat diffusion and radiation of each planetesimal. We call $\Theta(t, m, \varepsilon, \mathcal{W})$ (in $\mathrm{kg}^{-1}\mathrm{J}^{-1}\mathrm{s}^{-1}$) the rate of creation or annihilation of a planetesimal of mass m and energy ε, by discontinuous processes. This accounts for either the formation of a new body (with unique mass and energy) from the collision of two smaller planetesimals, or the "disappearance" of a body from the mass-energy space after its collision with another planetesimal. This rate is a function of time and of the dynamics of the planetesimals; e.g., the interaction of planetesimals depends on their effective collisional cross sections, which are related to their masses (i.e., to their radii or their gravity which, assuming that they have comparable densities, are simple functions of their masses). Mass and energy conservation laws require that $\Theta(t, m, e, \mathcal{W})$ is also a function of the distribution $\mathcal{W}(t, m, \varepsilon)$ itself (e.g., planetesimals that do not exist cannot disappear, thus $\Theta(t, m, \varepsilon, \mathcal{W})$ cannot be negative when $\mathcal{W}(t, m, \varepsilon) = 0$). On the contrary, radioactive decay and heat radiation change the energy of an isolated planetesimal and thus are continuous processes. We call $\dot{\varepsilon}(t, m, \varepsilon)$ the rate at which a planetesimal (m, ε) increases its internal energy. The evolution of the mass-energy distribution $W(t, m, \varepsilon)$ is governed by

$$\frac{\mathrm{d}\mathcal{W}}{\mathrm{d}t} + \frac{\partial \dot{\varepsilon}\mathcal{W}}{\partial \varepsilon} = \Theta. \tag{6}$$

This is akin to (3) with ε instead of m being a continuous variable. This equation (6) can be integrated over all possible energies. The total number of planetesimals dN between masses $m - \mathrm{d}m/2$ and $m + \mathrm{d}m/2$, whatever their energies (defined in eq.(1)), is related to dn by $\mathrm{d}N = \int_\varepsilon \mathrm{d}n = \mathrm{d}m \int_\varepsilon \mathcal{W} \mathrm{d}\varepsilon$ where the integration is over all possible energies. Therefore $\mathcal{W}$ and $\mathcal{V}$ are related by

$$\mathcal{V} = \int_\varepsilon \mathcal{W} \mathrm{d}\varepsilon, \tag{7}$$

and $\mathcal{V}$ is the marginal probability of $\mathcal{W}$. Similarly, the integration over all possible energies of Θ (the rate of creation/annihilation or a planetesimal of given mass and energy) is Γ (the rate of creation/annihilation or a planetesimal of given mass)

$$\Gamma = \int_\varepsilon \Theta \mathrm{d}\varepsilon. \tag{8}$$

The integration in energy of the second term of the left side of (6) is zero as it is $[\dot{\epsilon}\mathcal{W}]_{\epsilon=0}^{\infty} = 0$ ($\dot{\epsilon} = 0$ for $\epsilon = 0$ and there are no planetesimals of infinite energy). Therefore the equation (2) results from the integration over all energies of the equation (6).

3. Changes in thermal energy and number of planetesimals

3.1. Continuous change of thermal energy of a planetesimal

We define the thermal energy of each planetesimal

$$\varepsilon(t) = \int 4\pi r^2 \rho C \left(T(r, t) - T_\infty\right) \mathrm{d}r \tag{9}$$

where C is heat capacity, ρ density, T_∞ the background temperature in the nebula (numerical values are listed in Table 1) and $T(r, t)$ the radial temperature profile in the planetesimal at radius r and time t. In between collisions, the thermal energy of each planetesimal varies according to the heat equation

$$\dot{\varepsilon}(t) = \frac{\partial \varepsilon}{\partial t} = -\phi(t) + mH_0 e^{-t/\tau} \tag{10}$$

where $\phi(t) = 4\pi R^2 q(t)$ is the heat flow radiated at the surface of a planetesimal, $q(t)$ the time dependent local heat flow, H_0 the initial radioactive power content in W kg^{-1} and τ the radioactive decay time.

To solve the differential equation (10), we need to relate the heat flow $\phi(t)$ to the thermal energy $\epsilon(t)$. This can only be done approximately as it would be numerically impossible to monitor the temperature profile in each of the planetesimals that we want to consider (we will use typically 10^{24} planetesimals in our simulations). We therefore assume that the temperature in the planetesimals are self-similar with

$$T(r,t) = T_\infty + (T(0,t) - T_\infty) f(r/R) \tag{11}$$

where $T(0,t)$ is the central temperature of the planetesimals and where the boundary conditions are $f(0) = 1$, $f(1) = 0$. The self similarity of the thermal profile is a strong assumption that should be valid before planetesimals start to convect. Using (9) and (11) it is easy to compute that the thermal energy is

$$\varepsilon(t) = 4\pi\rho C(T(0,t) - T_\infty) R^3 \int_0^1 f(u) u^2 \, \mathrm{d}u \tag{12}$$

and the surface heat flow with $q = -k\mathrm{d}T/\mathrm{d}r|_{r=R}$

$$\phi(t) = -4\pi Rk(T(0,t) - T_\infty) f'(1) \tag{13}$$

where $f'(1)$ is the derivative of $f(u)$ for $u = 1$. The unknown temperature increase $T(0,t) - T_\infty$ can be eliminated between (12) and (13) and expressing R as a function of m, we write the heat equation as

$$\dot{\varepsilon}(t) = -a\left(\frac{4\pi\rho}{3}\right)^{2/3} \kappa\varepsilon(t) m^{-2/3} + mH_0 e^{-t/\tau} \tag{14}$$

where κ is the thermal diffusivity and a is the constant

$$a = f'(1) / \int_0^1 f(u) u^2 \, \mathrm{d}u. \tag{15}$$

The exact value of the constant a depends of course of the temperature profile and therefore of $f(u)$. However whether we assume that the temperature profiles are linear with the radius (i.e., $f(u) = 1 - u$), quadratic ($f(u) = 1 - u^2$) or cubic ($f(u) = 1 - u^3$), the resulting value of a is not very different as these choices lead to $a = 12$, $a = 15$ and $a = 18$, respectively. In our code we use $a = 15$ which corresponds to an assumed parabolic temperature profile in the planetesimals. This estimate of the diffusive heat flow is exact for a planet in steady state equilibrium.

In deriving this model of heat transfer we make various assumptions. First, we considered that the characteristic length of thermal diffusion is the planetesimal radius R. This holds until temperatures reach ≈1300 K and above, when the metal and then the silicates start melting and convecting (Agee et al., 1995; Hirschmann, 2000). At such large temperatures, the diffusive transfer of energy occurs through a boundary thickness δ. For example, Spohn & Schubert (1982) use, for a generic planet, $q(t) = k(T(0,t) - T_\infty)/\delta$ where $\delta \propto \mathrm{Ra}^{-1/3}$ is a function of the Rayleigh number, Ra, of the convecting planetesimal. This has not been done here but could be implemented by choosing a rheology for the planetesimals. The latent heat of melting could also be accounted for.

We also considered that planetesimal accretion occurs at constant background temperature T_∞. The temperatures arrived at from various nebular models (e.g., Morfill & Wood, 1989)

Parameters			
ρ	density	4028	kg m^{-3}
κ	diffusivity	$3. \times 10^{-6}$	m^2 s^{-1}
C	heat capacity	938	J K^{-1} kg^{-1}
H_0	initial radioactive power	1.5×10^{-7}	W kg^{-1}
$\tau_{1/2}$	^{26}Al half life	0.717	Myr
τ	^{26}Al decay constant	1.034	Myr
σ	Stefan-Bolzmann constant	5.67×10^{-8}	W m^{-2} K^{-4}
$15(4\pi\rho/3)^{2/3}\kappa$	see (14)	0.03	kg$^{2/3}$ s^{-1}

Table 1: Parameters used in the calculations following Sramek et al. (2012).

range from 1000 K decreasing to ≈ 300 K at 3 AU (Weidenschilling, 1988). We assume that the accretion occurs locally without a global drift of the planetesimals with respect to the sun. In this case, all the temperatures that we discuss later are in fact temperature differences with respect to T_∞ and when needed in numerical estimates we use $T_\infty = 300$ K.

At last we assume that the surface temperature remains equal to T_∞. This is reasonable because the heat flow of internal origin $q(t)$ is negligible in comparison to the equilibrium black-body radiation σT_∞^4 (σ is the Stefan-Boltzmann constant). The surface temperature of a planetesimal $T(R,t)$ must only be a few K above T_∞ to radiate its internal heat according to the heat flow balance

$$\sigma T(R,t)^4 = \sigma T_\infty^4 + q(t). \tag{16}$$

For example, a 500 km radius planetesimal (Vesta size) formed where the background temperature was $T_\infty = 300$ K only needed to have a surface temperature 15 K hotter than T_∞ to radiate the internal heat flow $q = \rho H_0 R/3$ (see numerical values in Table 1, and we will see later that this heat flow corresponding to that released at steady state by a planetesimal with a constant and uniform radioactive power is largely overestimated). For a planet, the difference between $T(R,t)$ and T_∞ is larger as it increases with the internal heat flow (proportional to R for a constant heat source), but the average temperature of a large body is mostly a function of its internal radioactivity and gravitational energy and not of its surface condition.

3.2. *Discontinuous changes of thermal energy during impact*

Assuming that two planetesimals of masses m_i and m_k and equal density ρ are attracted from an infinite distance by their respective gravities, their kinetic energy just before collision (assuming they can be considered as point masses) is

$$K = G\left(\frac{4\pi\rho}{3}\right)^{1/3} \frac{m_i m_k}{m_i^{1/3} + m_k^{1/3}} \tag{17}$$

During the collision, most of this kinetic energy is rapidly radiated away but some is buried in the resulting planet by the penetration of the impactor and the propagation and dissipation of a shock wave. A fraction f = 20-40% of the impactor kinetic energy is typically converted to thermal energy (depending of the impactor mass, obliquity of the impact, etc. see e.g. O'Keefe & Ahrens, 1977; Pierazzo & Melosh, 2000; Sramek et al., 2012). We therefore consider that a thermal energy $\Delta\varepsilon = fK$ with $f = 0.2$ is deposited in the newly formed planetesimal. The temperature increase mostly occurs in a volume beneath the impact point. However a large number of impacts occur randomly at the surface of each planetesimal in time intervals short compared to their accretion time. Therefore in our simple thermal model we can assume that this energy input is immediately redistributed throughout the whole planetesimal which then keeps its self similar and radially symmetric thermal profile. Mathematically, each impact corresponds in our model to a discontinuous increase of the temperature $T(0,t)$ of the planetesimal and of its radius R (see (11)).

The importance of impact heating depends of the rate of collision, however, a simple numerical estimate using (17) shows that until impactors reach 10^{20} kg ($\approx$ 181 km radius), the temperature increase due to the collision of planetesimals, $\Delta\varepsilon/(m_i+m_k)C$, is only 1.96 K. This thermal contribution increases very rapidly with the radius of impacted planetesimal and becomes the major cause of melting in planetary embryos. More precisely, the dissipation of the total kinetic energy of all the impactors that formed a planet of radius R or mass M (often called the gravitational energy of a planet, Solomon (1979), see also Sramek et al. (2010)) is associated with the temperature increase

$$\Delta T_g = f\frac{4\pi}{5}\frac{G\rho R^2}{C} = f\frac{3}{5}\left(\frac{4\pi\rho}{3}\right)^{1/3}\frac{GM^{2/3}}{C}. \tag{18}$$

In the following, we will show simulations of planet accretion starting from a swarm of total mass $M = 10^{24}$ kg. Therefore a source of gravitational potential energy which is able to raise the temperature by $\approx$2000 K is available if the simulation results in the formation of a single planet.

3.3. Changes of the planetesimal distribution

Although we are far from having discussed the necessary properties of $\Theta(t,m,\varepsilon,\mathcal{W})$ and the general solutions of equation (6), it is instructive to describe first how we deal numerically with the problem before presenting more theoretical considerations. The mathematical tools involve multiple integrals and distributions and therefore a level of complexity that obscures the physical simplicity of the process. The process is indeed straightforward and reflects the principle of the Smoluchovski aggregation with a drift term:

1. Jump: in the mass-energy distribution, we consider the planetesimals (m_1,ε_1) and (m_2,ε_2); if they merge at time t, we remove them from their respective distributions (i.e., subtract 1 each from $\mathcal{W}(t,m_1,\varepsilon_1)$ and from $\mathcal{W}(t,m_2,\varepsilon_2)$) and add a new planetesimal $(m_1+m_2,\varepsilon_1+\varepsilon_2+\Delta\varepsilon)$ to the appropriate distribution (i.e., add 1 to $\mathcal{W}(t,m_1+m_2,\varepsilon_1+\varepsilon_2+\Delta\varepsilon)$ as mass is conserved and as thermal energy can be increased by impact heating $\Delta\varepsilon$).
2. Drift: during a time step dt, each planetesimal changes its energy continuously, so that each planetesimal (m,ε) leaves the distribution to be reintroduced as $(m,\varepsilon+\dot{\varepsilon}\mathrm{d}t)$ (i.e., subtract 1 from $\mathcal{W}(t,m,\varepsilon)$, and add 1 to $\mathcal{W}(t,m,\varepsilon+\dot{\varepsilon}\mathrm{d}t)$)

The numerical code corresponding to this process, generalizes in the $m-\varepsilon$ space what has been used in Inaba et al. (1999, 2001) following Wetherill (1990). We sample the $m-\varepsilon$ space in $[i,j]$ bins; each bin contains N_{ij} planetesimals with masses between $\mathcal{M}_i$ and $\mathcal{M}_{i+1}$ and energies between $\mathcal{E}_j$ and $\mathcal{E}_{j+1}$ (see Fig. 1). The total mass of all the planetesimals of the bin $[i,j]$ is M_{ij} and their total energy is E_{ij}, so that each planetesimal of the bin $[i,j]$ has, on average, a mass m_{ij} with $\mathcal{M}_i \le m_{ij} \le \mathcal{M}_{i+1}$,

$$m_{ij} = \frac{M_{ij}}{N_{ij}} \tag{19}$$

and an energy ε_{ij} with $\mathcal{E}_j \leq \varepsilon_{ij} \leq \mathcal{E}_{j+1}$,

$$\varepsilon_{ij} = \frac{E_{ij}}{N_{ij}} \tag{20}$$

We call $\Lambda(i, j, k, l)$ (in s^{-1}) the rate at which planetesimals in bins $[i, j]$ and $[k, l]$ can merge. It seems reasonable to assume that the rates of collision are functions of the planetesimal cross sections related to their radii and masses, not of their internal energies (although, one may argue that the sticking efficiency of a planetesimal collision may be affected by their thermal energies, see Wettlaufer (2010)). We therefore consider that $\Lambda(i, j, k, l)$ is only a function of the the masses m_{ij} and m_{kl} of the colliding planetesimals) and write it $\Lambda(m_{ij}, m_{kl})$. The rate $\Lambda(m_{ij}, m_{kl})$ is usually call the "coagulation kernel" (e.g. Wetherill, 1990; Collet, 2004).

The number of collisions during the time step dt, between the planetesimals of two different interacting bins is

$$\mathrm{d}N = N_{ij} N_{kl} \Lambda(m_{ij}, m_{kl}) \mathrm{d}t. \tag{21}$$

Planetesimals can also coalesce with planetesimals from the same bin in which case

$$\mathrm{d}N = \frac{1}{2} N_{ij}(N_{ij} - 1)\Lambda(m_{ij}, m_{ij})\mathrm{d}t \tag{22}$$

(a given planetesimal cannot merge with itself and the factor of $1/2$ precludes counting $[i, j]$ and $[k, l] = [i, j]$ as two different populations). Therefore using a Kronecker symbol δ_{ij} (unity for $i = j$, and zero otherwise), we have, in the general case, dN collisions between bins $[i, j]$ and $[k, l]$ with

$$\mathrm{d}N = \frac{N_{ij}(N_{kl} - \delta_{ik}\delta_{jl})}{1 + \delta_{ik}\delta_{jl}} \Lambda(m_{ij}, m_{kl})\mathrm{d}t. \tag{23}$$

The merging of the planetesimals $(m_{ij}, \varepsilon_{ij})$ and $(m_{kl}, \varepsilon_{kl})$ results in a planetesimal $(m_{pq}, \varepsilon_{pq})$ belonging to the bin $[p, q]$ (i.e., $\mathcal{M}_p \leq m_{ij} + m_{kl} < \mathcal{M}_{p+1}$ and $\mathcal{E}_q \leq \varepsilon_{ij} + \varepsilon_{kl} + \Delta\varepsilon < \mathcal{E}_{q+1}$). Therefore, in the bin $[i, j]$ we remove dN planetesimals, decrease the total mass by $m_{ij}\mathrm{d}N$ and the total energy by $\varepsilon_{ij}\mathrm{d}N$, in the bin $[k, l]$ we also remove dN planetesimals, decrease the total mass by $m_{kl}\mathrm{d}N$ and the total energy by $\varepsilon_{kl}\mathrm{d}N$, while in the bin $[p, q]$ we add dN planetesimals, and increase the total mass by $(m_{ij} + m_{kl})\mathrm{d}N$ and the total energy by $(\varepsilon_{ij} + \varepsilon_{kl} + \Delta\varepsilon)\mathrm{d}N$. Notice that the bin $[p, q]$ can be identical to the bin $[i, j]$ that contained the largest planetesimals when a large target receives a small impactor (see green dots in Fig. 1)

During the time dt, the energy ε_{ij} of a planetesimal belonging to the bin $[i, j]$ changes continuously by $d\varepsilon_{ij}$

$$\mathrm{d}\varepsilon_{ij} = \dot{\varepsilon}(t, m_{ij}, \varepsilon_{ij})\mathrm{d}t. \tag{24}$$

This change of energy brings these planetesimals to the bin $[i, k]$ (the mass bin i does not change but they move to the energy bin k where $\mathcal{E}_k \leq \varepsilon_{ij} + \mathrm{d}\varepsilon_{ij} \leq \mathcal{E}_{k+1}$). We therefore remove the N_{ij} planetesimals, with their total mass M_{ij} and total energy E_{ij} from the bin $[i, j]$ and add these N_{ij} planetesimals, with their total mass M_{ij} and total energy $E_{ij} + N_{ij}\mathrm{d}\varepsilon_{ij}$ in the bin $[i, k]$. The bin $[i, k]$ may or may not be the same as the bin $[i, j]$ (see the blue and purple dots of Fig. 1).

Although this redistribution of the planetesimals in the (m, ε) space may seem convoluted, it is simple to code. A difficulty is the fact that the number of planetesimals is an integer number. The number of collisions dN is rounded to the integer below or above using a random function so that we only form an integer number of planetesimals and never a fraction of planetesimal,

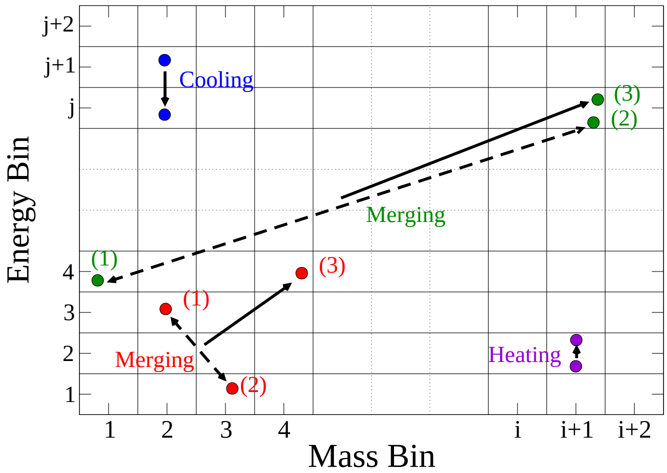

Figure 1: Evolution of $\mathcal{W}(m, \varepsilon)$ in the $m - \varepsilon$ space during discontinuous and continuous processes. Two planetesimals (m_1, ε_1) and (m_2, ε_2) can collide and merge to form the new planetesimal (m_3, ε_3) (red and green). The new planetesimal has a mass $m_3 = m_1 + m_2$ and an energy $\varepsilon_3 = \varepsilon_1 + \varepsilon_2 + \Delta\varepsilon$. Between the episodes of collision, the thermal energy of the planetesimal can also decrease by diffusion and radiation or increase by internal radioactivity decay (blue and purple). The final bin is sometimes identical to the initial bin (green or purple cases).

which would be unphysical. To choose the time stepping dt we compute the changes dN_{ij} (which are proportional to dt, at least if one neglects the random rounding of numbers) in the bins that contain N_{ij} planetesimals and impose

$$\max\left(\frac{-\mathrm{d}N_{ij}}{0.1(N_{ij}-1)+1}\right) = 1 \quad \text{for } \mathrm{d}N_{ij} < 0 \tag{25}$$

so that, when N_{ij} is large, the number of planetesimals that can be removed from the bin $[i, j]$ is at most 10% of the population, but in the case where there is just 1 planetesimal in the bin $[i, j]$, it can be removed.

Finally, because of the exponential nature of the aggregation process, we use an exponential distribution of the bins for the mass (i.e., the mass bin i corresponds to the interval in kg, $[\delta^{i-3/2}, \delta^{i-1/2}]$ with $\delta = 1.15$ (starting from 1 kg pebbles to built an embryo of $O(10^{20})$ kg, the maximum number of mass bin i_{max} must be at least 330). Instead of discussing our results in terms of thermal energies, we rather present our results in terms of temperature excess, i.e., $\varepsilon_{ij}/(m_{ij}C)$ and for the temperature description we sometimes use a linear distribution for the temperature bins $\Delta T[j-3/2, j-1/2]$, with a temperature interval ΔT of typically 5 K , sometimes an exponential distribution in K, $[\delta^{j-3/2}, \delta^{j-1/2}]$ (with typically $\delta = 1.15$, the first interval is replaced by $[0, \sqrt{\delta}]$). The code being barely four embedded loops explores $(i_{max} \times j_{max})^2$ combinations per iteration in time (i_{max} and j_{max} are maximum number of bins in mass and energy), we try to keep $i_{max} \times j_{max}$ reasonably small to run a simulation in less than a few days on our standard workstation.

3.4. Remarks on dimensions

We write $\Lambda(m, m') = c\tilde{\Lambda}(\tilde{m}, \tilde{m}')$ where $\tilde{\Lambda}$ is a dimensionless function of the dimensionless masses $\tilde{m} = m/m_0$ and $\tilde{m}' = m'/m_0$ where m_0 is the mass of the smallest planetesimals. In this case, the constant c is in s^{-1}. We then normalize the number of planetesimal of a given size by N_0, the initial total number of planetesimals, and rewrite (23) as

$$\mathrm{d}\tilde{N} \approx \frac{\tilde{N}_{ij}\tilde{N}_{kl}}{1 + \delta_{ik}\delta_{jl}} \tilde{\Lambda}(\tilde{m}_{ij}, \tilde{m}_{kl})\,\mathrm{d}\tilde{t}. \tag{26}$$

(neglecting the very small $\delta_{ik}\delta_{jl}/N_0$) where we have defined the non-dimensional time $\tilde{t} = cN_0 t$, wherein $1/(cN_0)$ becomes the intrinsic time scale. Normalizing ε by $m_0 H_0/(cN_0)$, the energy evolution (14) becomes

$$\frac{\mathrm{d}\tilde{\varepsilon}}{\mathrm{d}\tilde{t}} = -A\tilde{\varepsilon}\tilde{m}^{-2/3} + \tilde{m}e^{-\tilde{t}/\tilde{\tau}} \tag{27}$$

where all the variables with tilde are non dimensional and

$$A = 15\left(\frac{4\pi\rho}{3m_0}\right)^{2/3} \frac{\kappa}{cN_0} \text{ and } \tilde{\tau} = cN_0\tau \tag{28}$$

We can therefore explore our parameter space by choosing the time scale $1/(cN_0)$ and the initial mass m_0 of the smaller planetesimals assuming their density and thermal diffusivity are known. The joint mass-temperature distribution depends on the choices of the aggregation kernel, the time scale and the mass of the smallest pebbles. However, the mass distribution integrated in energy $\mathcal{V}$ only depends on the aggregation kernel as (26) does not include any other free parameter.

3.5. Continuous representation of the changes of the planetesimal distribution

Although the numerical implementation of the equations that we have discussed may suffice, a few useful properties can be derived by using a continuous representation of the mass and energy distribution. This representation will also make the connection with the classic Smoluchovski formalism (von Smoluchowski, 1917) and with other results (Collet & Goudon, 2000; Collet, 2004; Leyvraz, 2005).

A new planetesimal (m, ε) can be formed by merging the planetesimal (m', ε') with $m' < m$ with the complementary planetesimal $(m", \varepsilon")$ with $m" = m - m'$, and $\varepsilon" = \varepsilon - \varepsilon' - \Delta\varepsilon$. The rate of merging is therefore related to the product of the number of planetesimals of mass and energy of both (m', ε') and $(m - m', \varepsilon - \varepsilon' - \Delta\varepsilon)$ times the rate of reaction $\Lambda(m', m - m')$ between these two populations. We assume this rate to be independent of the energies and only related to their masses. The increase of planetesimal population due to planetesimal merging is therefore

$$\Theta_1(m, \varepsilon) = \frac{1}{2}\iint \Lambda(m', m - m')\mathcal{W}(m', \varepsilon')\mathcal{W}(m - m', \varepsilon - \varepsilon' - \Delta\varepsilon)\,\mathrm{d}m'\mathrm{d}\varepsilon' \tag{29}$$

where the dependence on t is implicit. The integrals are over all possible masses and energies where the quantities of (29) are defined and the factor $1/2$ takes into account the fact that the same merging pair is counted two times (i.e. as $(m', \varepsilon') - (m", \varepsilon")$ and as $(m", \varepsilon") - (m', \varepsilon')$).

Of course, in this merging process, the number of planetesimals in the bin $[m, \varepsilon]$ decreases at the rate $\Theta_2(m, \varepsilon)$ because these planetesimals merge with over planetesimals in the bin $[m', \varepsilon']$ and thus leave their original bin. The rate of decrease is related to the number of planetesimals in $[m, \varepsilon]$ times the number of planetesimals in $[m', \varepsilon']$ times their rate of interaction $\Lambda(m, m')$,

$$\Theta_2(m, \varepsilon) = -\iint \Lambda(m, m')\mathcal{W}(m, \varepsilon)\mathcal{W}(m', \varepsilon')\, \mathrm{d}m'\mathrm{d}\varepsilon' \tag{30}$$

The total rate of planetesimal exchange through discontinuous process is therefore the sum $\Theta = \Theta_1 + \Theta_2$. This sum generalizes the coagulation equations proposed by von Smoluchowski (1917) to include energy distributions, and a symmetrical relation for it can also be derived, similar to what is obtained in Leyvraz (2005):

$$\Theta = \frac{1}{2}\iiiint R(m', m", \varepsilon', \varepsilon")D(m, m', m", \varepsilon, \varepsilon', \varepsilon")\, \mathrm{d}m'\mathrm{d}m"\mathrm{d}\varepsilon'\mathrm{d}\varepsilon" \tag{31}$$

where

$$\begin{aligned} R &= \Lambda(m', m")\mathcal{W}(m', \varepsilon')\mathcal{W}(m", \varepsilon") \\ D &= \delta(m - m' - m")\delta(\varepsilon - \varepsilon' - \varepsilon" - \Delta\varepsilon) - \delta(m - m')\delta(\varepsilon - \varepsilon') - \delta(m - m")\delta(\varepsilon - \varepsilon"). \end{aligned} \tag{32}$$

In this last expression δ is the Dirac distribution. This complex expression simply summarizes with a continuous representation what we have discussed in the presentation of the numerical implementation.

The integral of the three Dirac delta-functions of D containing energies, over all possible energies ε in (32), are each time 1, and therefore the evolution of the distribution integrated over all possible energies satisfies (2) with

$$\Gamma = \int \Theta \mathrm{d}e = \frac{1}{2}\iint \widetilde{R}(m', m")\widetilde{D}(m, m', m")\mathrm{d}m'\mathrm{d}m" \tag{33}$$

where

$$\begin{aligned} \widetilde{R} &= \Lambda(m', m")\mathcal{V}(m')\mathcal{V}(m") \\ \widetilde{D} &= \delta(m - m' - m") - \delta(m - m') - \delta(m - m"). \end{aligned} \tag{34}$$

This is exactly equivalent to the classic coagulation equations of Smoluchowski, (2) (von Smoluchowski, 1917; Leyvraz, 2005). Using the continuous expressions (31)-(32), we verify in the Appendix that our formalism conserves mass, leads to a decrease in the number of planetesimals, and provides an expression for the evolution with time of the total thermal energy of the swarm.

4. Benchmark test: thermal "mixing" of a swarm with $\Lambda(m, m') = cmm'$

4.1. Analytical solutions

Although no analytic solutions for a mass-energy distribution $\mathcal{W}$ satisfying (6), (31) and (32) exist, a few solutions are known for mass distribution $\mathcal{V} = \int \mathcal{W}\,\mathrm{d}e$ when Λ is simple enough, i.e., when $\Lambda(m, m') = c$, $\Lambda(m, m') = c(m + m')$, or $\Lambda(m, m') = cmm'$ and c constant (von Smoluchowski, 1917; Safronov, 1962; Trubnikov, 1971; Wetherill, 1990; Collet & Goudon, 2000).

These solutions assume that all the planetesimals are formed by the successive coalescence of planetesimals of initial, identical masses m_0, so that all planetesimals have a mass multiple of m_0 and that the nondimensional kernels of the interaction of planetesimals of nondimensional masses i and j are $\Lambda_{ij} = 1, i + j$ or $i \times j$. The number n_k of planetesimals of mass km_0 is therefore

$$\frac{\mathrm{d}n_k}{\mathrm{d}t} = \frac{1}{2}\sum_i \sum_j \Lambda_{ij} n_i n_j (\delta(k-i-j) - \delta(k-i) - \delta(k-j)) = \frac{1}{2}\sum_{i+j=k} \Lambda_{ij} n_i n_j - n_k \sum_i \Lambda_{ik} n_i. \quad (35)$$

This equation is the discrete equivalent of (31) integrated in energy, see (33). We refer to Collet & Goudon (2000) or Leyvraz (2005) for the details of finding solutions, but we can briefly sketch the method here. First, we note that when $\Lambda_{ik} = 1$, the last term of (35) is $\sum_i \Lambda_{ik} n_i = \sum_i n_i = N(t)$ where $N(t)$ is the total number of objects, which is a known quantity because according to (A.6), $\dot{N}(t) = -(c/2)N(t)^2$. Similarly this last term of (35) is also known when $\Lambda_{ik} \propto i$ as $\sum_i \Lambda_{ik} n_i \propto \sum_i i n_i = M_0$ the total mass of planetesimals, which is constant (the nondimensional total mass is also the initial number of pebbles N_0). Therefore when $\Lambda_{ij} = 1$, $\Lambda_{ij} = i + j$, or $\Lambda_{ij} = i \times j$, the sum appearing in the last term of (35) is analytically known and the solution can be found by recurrence as the evolution of n_k is only related to the total mass (a constant), the total number of planetesimals (known, see A.6) and the number of planetesimals of masses smaller than k. The discrete equation (35) or its continuous equivalent (2), (33) and (34) have therefore been solved analytically in the three cases described above and numerically in other cases.

In a physical problem with no intrinsic length scale, solutions can be searched on the form of self similar expressions and therefore assuming

$$\mathcal{V}(t, m) = F(t) G\left(\frac{m}{\overline{m}(t)}\right) \quad (36)$$

where $\overline{m}(t)$ is the average mass of the planetesimals at time t and G a shape function. The conservation of the mass of the planetesimal swarm (i.e., the conservation of $\int m\mathcal{V}\,\mathrm{d}m$) readily implies that the amplitude $F(t)$ is proportional to $\overline{m}(t)^{-2}$. By plugging the expression (36) into (2), (33) and (34), self similar solutions can be found after some algebra (see Ricard & Bercovici, 2009). In the case where $\Lambda(m, m')$ varies like $(m + m')^\alpha$ or $(mm')^{\alpha/2}$, it can be shown that $\mathrm{d}\overline{m}/\mathrm{d}t$ must be proportional to $\overline{m}^\alpha$. When α is 0, 1, or 2 (e.g., when $\Lambda(m, m') = c$, $c(m + m')$ or cmm'), self similar solutions if they exist, imply that the average mass of the planetesimals $\overline{m}$ increases like $m_0 + a_0 t$, $m_0 \exp(a_1 t)$ and $m_0/(1 - a_2 t)$ respectively (with a_0, a_1 and a_2 constants). In the following, we will also discuss the cases $\Lambda = c(m+m')^{2/3}$ and $c(m+m')^{4/3}$ which should have self similar solutions with $\overline{m}$ varying like $m_0 + a_4 t^3$ and $m_0/(1 - a_5 t^3)$ (with a_4 and a_5 constants). The existence of self similarity implies that $m^2\mathcal{V}(t, m) \propto u^2 G(u)$ plotted as a function of $u = m/\overline{m}(t)$ is independent of time, and plotted as a function of m looks like propagating as a function of time (or of $\overline{m}(t)$ which is an increasing function of time, Ohtsuki et al. (1990), Wetherill (1990)).

The existence of self similar solutions for (2) does not mean that these solutions are indeed chosen in a naturally evolving situation. In fact, these self similar solutions are the correct ones only in the case $\alpha < 1$; this corresponds to what Wetherill called an *orderly growth* of the planetesimal swarm. When $\alpha > 1$ the average mass seems surprisingly to reach infinity after a finite time which is obviously absurd as $\overline{m}$ is necessarily bounded by the initial mass of the swarm. What happens in these cases, is a phenomenon called "gelation". After a critical time, the mass distribution splits and a single large body escapes from the continuous distribution. This "runaway" planetesimal is known to be formed during planet accretion and the critical time at which it is formed defines the early stage of *runaway growth* to the later stages of *oligarchic growth* where several planet embryos interact (Kortenkamp et al., 2000).

As the formation of planets occurred in a runaway process, it involved a coagulation kernel where masses appeared with a power α larger than 1. We therefore benchmark our code in the case $\Lambda(m, m') = cmm'$ with the analytic non-dimensional solution found when $\Lambda_{ij} = i \times j$. According to Trubnikov (1971), the number n_k of planetesimals of mass k is

$$n_k = N_0 \frac{k^{k-2}}{k!} t^{k-1} \exp(-kt) \approx N_0 \frac{\exp(k)}{\sqrt{2\pi k^5}} t^{k-1} \exp(-kt) \tag{37}$$

where the approximation makes use of Stirling's formulae (i.e., the approximation of a factorial for large numbers). This solution is valid until the runaway occurs at $t = 1$. At this time, a single runaway planet is formed and leaves a swarm of small planetesimals with a distribution still given by (37) (i.e., (37) remains correct except that it misses a single large planetesimal when $t > 1$; see e.g., Wetherill, 1990).

4.2. Mixing two populations with $\Lambda(m, m') = cmm'$ and $\dot{\varepsilon} = 0$

We choose as a benchmark test, $\Lambda(m, m') = cmm'$ with arbitrarily $cN_0 = 1$ Myr^{-1}. This is similar to what has been used in Wetherill (1990) and the critical time for the onset of runaway is $1/(cN_0) = 1$ Myr. We assume $\dot{\varepsilon} = 0$ but start from $N_0 = 10^{24}$ planetesimals with equal masses (1 kg) where half of them are cold ($T_1 = 0$ K) and half of them hot ($T_2 = 1000$ K). We therefore study the mixing of these two populations and not surprisingly we expect that the accretion will lead to planetesimals of intermediate temperatures.

Starting from a distribution where all planetesimals have the same mass, our test simulation must lead to a distribution $\mathcal{W}(t, m, \varepsilon)$ which, when integrated over energy, corresponds to (37). Specifically, n_k in (37) is the number of planetesimals of mass km_0, while in our numerical code we compute a number of planetesimals N_{kj} in bins of finite dimensions, where j is an energy bin and k the mass bin of width Δm_k that includes km_0, thus, one expects that when $\Delta m_k > 1$, $\sum_j N_{kj} \approx n_k \Delta m_k$.

In Figure 2a, we plot the total number of planetesimals per mass interval whatever their thermal energies (i.e. $\sum_j N_{kj}/\Delta m_k$) at various times. The results are similar to those depicted by Wetherill (1990, Fig. 5) and in close agreement with (37). The initial distribution (a Dirac δ at $t = 0$), becomes wider until $t \geq 1$ Myr where a single embryo is formed reaching already a size of 10^{17} kg at $t = 1.006$ Myr. This embryo and its evolution cannot be plotted on the same graph (too large abscissae and too small ordinate). Simultaneously the remaining continuous distribution of sizes (with masses smaller than $\approx 10^6$ kg) starts to shrink as the planetesimals fall on the runaway embryo. The total number of planetesimals per mass interval varies as $m^{-5/2}$ around the critical time $t = 1$ Myr(Trubnikov, 1971). The total number of planetesimals (Figure 2b) decreases linearly with time until $t = 1$ Myr (as the average planetesimal mass increases as $1/(1 - a_2 t)$ for the kernel $\Lambda(m, m') = cmm'$, before the embryo runaway); after $t = 1$ Myr, it decreases exponentially with time (Wetherill, 1990).

The novelty of our model is in the joint evolution of mass and temperature distributions, which describes the mixing and aggregation of the two original populations (See Fig. 3). The distribution in mass-temperature space remains symmetric with respect to the average initial temperature (Fig. 3). The distribution of planetesimal temperatures is shown in Figure 4. A number of planetesimals of a few m_0 masses and temperatures of order $(n_1 T_1 + n_2 T_2)/(n_1 + n_2)$ where n_1 and n_2 are small integer numbers are rapidly formed. Not surprisingly, the runaway embryo formed at $t \approx 1$ Myr has the average temperature of the two original swarms. The embryo contains already $\approx 50\%$ of the total initial mass at $t = 1.68$ Myr (Fig. 3e). A large

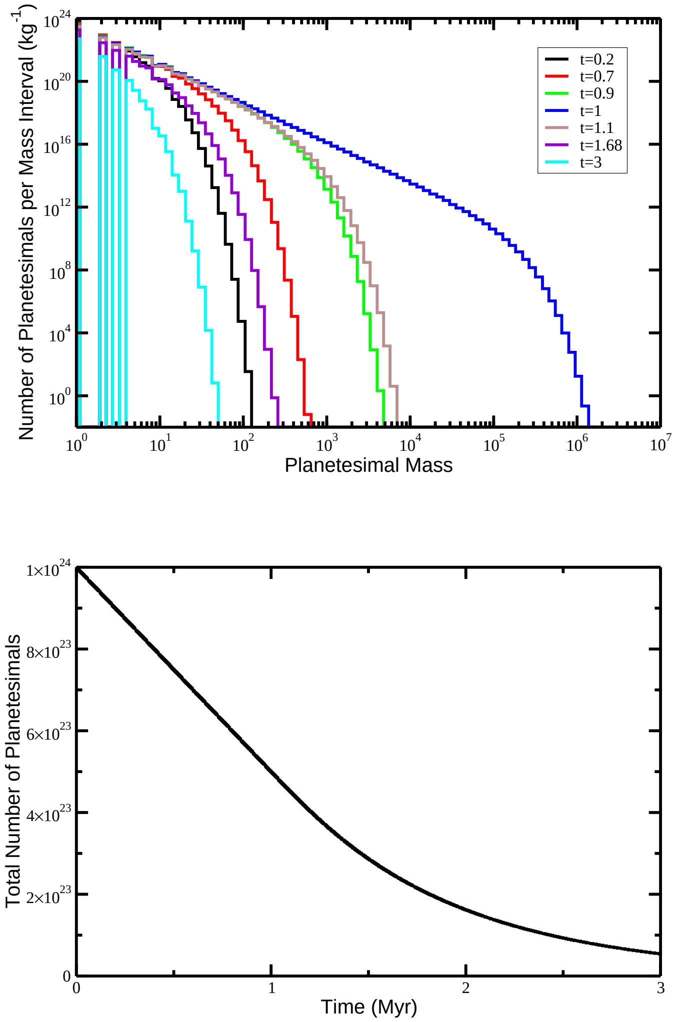

Figure 2: Panel a: Evolution of the number of planetesimals per mass interval when the rate of merging is $\Lambda(m, m') = cmm'$. The simulation starts with $N_0 = 10^{24}$ identical planetesimals. Some bins with low masses are empty as the merging of planetesimals of mass m_0 cannot give a planetesimal of mass smaller than $2m_0$ which populates the 7th bin (we use $\delta = 1.15$ and $\delta^{7-3/2} \leq 2 \leq \delta^{7-1/2}$). At $t = 1$ Myr, in agreement with the analytical solution, the distribution of planetesimals becomes discontinuous and a single runaway embryo is formed (not shown). After the embryo is formed, the number of small planetesimals decreases at they fall onto the runaway embryo, with the population of large planetesimals being depleted first. Panel b: Total number of planetesimals as a function of time. This number decreases linearly with time until the runaway embryo is formed (at $t = 1$ Myr), later the decrease becomes exponential (Wetherill, 1990).

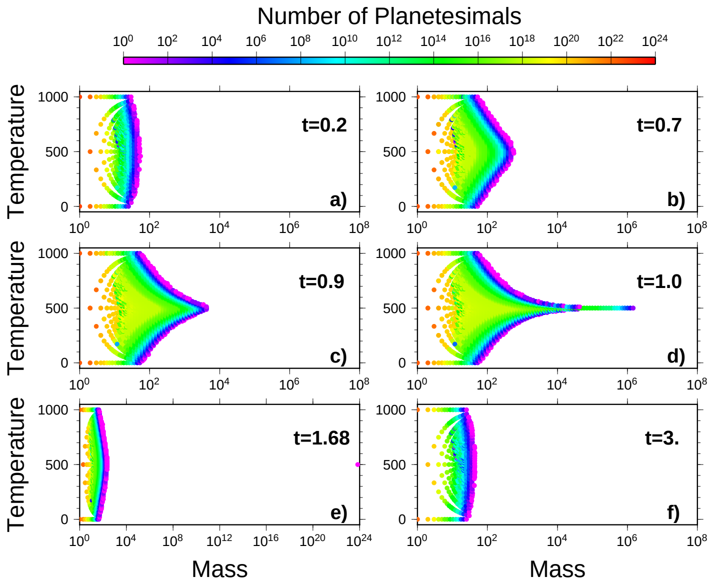

Figure 3: Joint mass-temperature distribution of planetesimals at different times, for the rate of merging $\Lambda(m, m') = cmm'$. We neglect radioactivity and heat diffusion. The swarm of planetesimals at $t = 0$ is made of two populations with temperatures 0 and 1000 K. The number of planetesimals per mass bin, integrated for all possible temperatures, is depicted in Figure 2. The number of planetesimals per temperature bin, integrated for all possible sizes, is depicted in Figure (4). Not surprisingly, the largest planetesimals, and the subsequent planet embryo, have approximatively the average temperature 500 K. The slight dissymmetry of the distribution with respect to the average distribution is rather introduced by the plotting method than by the stochastic rounding of our code. In the panel (e), we changed the horizontal scale to show the large runaway embryo of mass $\approx 5 \times 10^{23}$ kg that has been formed.

number of very small planetesimals still survive at $t = 3$ Myr, slowly falling on the embryo (Fig. 3f).

5. Temperature evolution of a swarm of planetesimals

5.1. The aggregation kernels

As our code has now been benchmarked we can use it for more realistic simulations. Terrestrial planets were formed by settling of dust toward the mid-plane of a solar nebula. Before km-size planetesimals were formed, the gravitational attraction of the planetesimals themselves was negligible. Gas was present in the nebula and there was a mass-dependent difference between the velocities of refractory nebular masses (Whipple, 1964; Nakagawa et al., 1986; Youdin, 2010). While the larger bodies (with sizes $\geq$ 10 m) maintained mostly Keplerian orbits, the smallest grain-sized bodies (say $\leq$ 1 cm in size) were primarily swept along by the gas rotation and had smaller orbital velocities. This favored the growth of the largest grains that were gathering more slowly moving dust and smaller grains. This period of growth of small bodies could have been

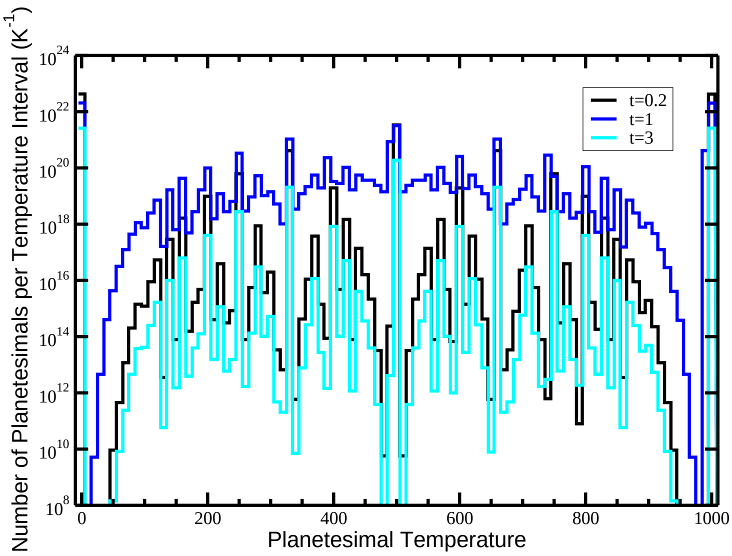

Figure 4: Temperature distribution of planetesimals at times 0.2, 1 and 1.68 Myr corresponding the mass-temperature distributions of Figure (3), panels (a), (d) and (e).

favored by gravitational instabilities in the planetary disk as a whole, at least if the turbulent motions that might have been induced in the disk by shearing instabilities between the disk and the gas above and below it, were not too large (Wetherill, 1990). The coagulation of dust or grains requires the presence of some stickiness between the grains whose physical basis is debated (Wettlaufer, 2010).

A planetesimal of radius R and mass M, orbiting the proto-Sun with a relative velocity V_{rel}, sweeps through the volume per unit time $\dot{\Omega} = \pi R'^2 V_{rel}$ where $R' \geq R$ as gravitation draws in other planetesimals. An impactor reaching tangentially this planetesimal with an impact velocity V_i has an angular momentum$V_i R$ and comes from the distance R', radial to the planetesimal trajectory such that $V_i R = V_{rel} R'$. As by energy conservation $V_i^2 = V_{rel}^2 + V_{esc}^2$, where the gravitational escape velocity is

$$V_{esc} = \sqrt{\frac{2GM}{R}} = \sqrt{2G}\left(\frac{4\pi\rho}{3}\right)^{1/6} M^{1/3}, \tag{38}$$

a planetesimal orbiting the proto-Sun sweeps through the volume per unit time

$$\dot{\Omega} = \pi R'^2 V_{rel} = \pi R^2 \left[1 + \left(\frac{V_{esc}}{V_{rel}}\right)^2\right] V_{rel}. \tag{39}$$

The typical relative velocity of a dust grain is V_{rel} =1-50 m s^{-1}, thus planetesimals need to reach masses $M \approx 10^{16}$ kg (i.e., radius R of order 10 km) for their gravitational escape velocity, V_{esc} to exceed V_{rel}. The rate at which a small planetesimal ($R << 10$ km) can grow, related to the volume it sweeps per unit time is $\dot{\Omega} \approx \pi R^2 V_{rel}$, which is itself proportional to its mass to the $2/3$ power. This suggests that a coagulation kernel of the form $\Lambda(m, m') \propto (m + m')^{2/3}$ might be a reasonable proxy for the first phase of coagulation (Wetherill, 1990). This initial phase does not lead to the formation of a runaway planetary embryo since the kernel has a power $2/3$ smaller than 1.

During this initial phase, radioactivity is very inefficient at warming up planetesimals. A 1-km body has a diffusion time $t_D \approx R^2/\kappa$ of only $\approx$10 kyr. If the body accretes in a time smaller than t_D (i.e., $t \leq t_D << \tau$), then its maximum temperature increase is lower than

$$T_H = \frac{H_0 \tau}{C}(1 - e^{-t/\tau}) \approx \frac{H_0 t}{C} \approx 50 \text{ K}, \tag{40}$$

neglecting diffusion. If it accretes in a time larger than t_D, then its maximum temperature increase is lower than

$$T_E = \frac{H_0 R^2}{6\kappa C} \approx 8.6 \text{ K}, \tag{41}$$

which would be the maximum temperature of a planetesimal in thermal steady state equilibrium with a uniform and constant radiogenic heating H_0. These estimates, either (40) or (41), show that km-size planetesimals cannot reach high temperatures. It is only when they reach tens of kilometers that they may become hot enough to melt, but then the kinetic energy due to impacts cannot be neglected.

As a large planetesimal orbits the proto-Sun, it sweeps through a volume dominated by its effective gravitational cross-section, which is a function of relative and escape velocities – i.e., $\dot{\Omega} \approx \pi R^2 V_{esc}^2 / V_{rel}$. Therefore, since both R and V_{esc} are proportional to $M^{1/3}$, a coagulation kernel of the form $\Lambda(m, m') \propto (m + m')^{4/3}$ gives a reasonable proxy for a second phase of coagulation that involves gravitational focussing (Wetherill, 1990). This second phase leads to a runaway growth of planetesimals forming a limited number of planetary embryos of lunar or Martian masses, say 10^{22} – 10^{23} kg (see e.g. Kortenkamp et al., 2000). During this period, the source of heating is still radiogenic but the dissipation of kinetic energy during the impacts becomes an increasingly significant heat source.

The use of coagulation kernels with masses to the powers $2/3$ or $4/3$ is a relatively crude approximation of the real physics of accretion. The relative velocity V_{rel} in (39) should itself be a function of the dynamics of the planetesimal formation (see e.g., Stewart & Wetherill, 1988; Wetherill & Stewart, 1989). However we will use these simple kernels corresponding to situations with or without runaway growth in order to focus on the implications for the temperature distribution of planetesimals.

In the last phase of oligarchic growth, the successive collisions and merging of planetary embryos leads to the formation of planets like our solar-system's current planets via giant impacts. This late stage is accessible to models, wherein the trajectories can be computed exactly (Morbidelli et al., 2009). In this case, dissipation of kinetic energy during impacts is the major source of heating (with the minor addition of core-mantle differentiation, Ricard et al., 2009)); by this time radiogenic heating from ^{26}Al decay becomes negligible, while the heating by slowly decaying elements (U, Th, K) has yet to become significant.

5.2. Non-gravitational coagulation

Assuming that a $\Lambda = c(m + m')^{2/3}$ kernel is a reasonable guess for the earlier stages of planetesimal formation, we perform various simulations with different time constants, starting

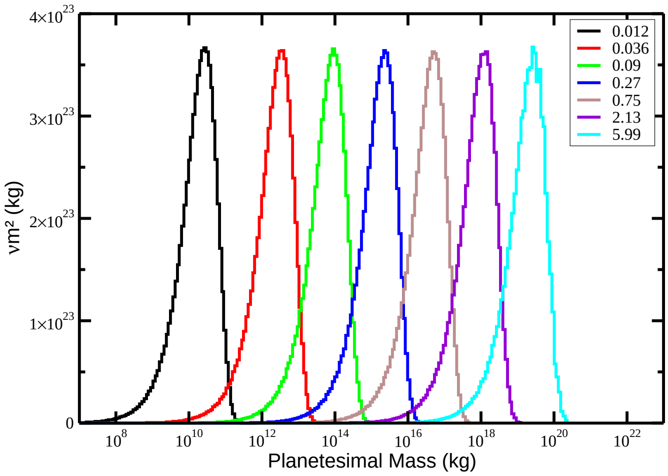

Figure 5: Mass distributions multiplied by m^2 plotted as a function of planetesimal masses for different dimensionless times (these times are indicated in Myr). As the aggregation kernel $\Lambda(m, m') \propto (m + m')^{2/3}$ has a mass exponent smaller than 1, the distribution is self similar with an average mass $\bar{m}(t)$ increasing with $\tilde{t}^3$.

from a swarm of net mass $M_0 = 10^{24}$ kg made of 10^{24} pebbles of sizes 1 kg. As already discussed, the mass distribution as a function of dimensionless time, integrated in energy, does not depend on heat production or dissipation. For a kernel with a mass exponent smaller than 1, the solutions become rapidly self similar; i.e. $m^2\mathcal{V}(t, m) = m^2 \int \mathcal{W}(t, m, e)\mathrm{d}e$ is a function of $m/\bar{m}(t)$ and with the same shape for all time (Fig. 5). The self-similarity of the mass distribution is obvious in Figure 5: the discrete and stochastic nature of this distribution becomes evident at the largest time when the number of planetesimals in the bins becomes small. The mass distributions $\mathcal{V}(t, m)$ are simple decreasing functions of m (like in the case depicted in Figure 2).

We perform simulations with the same non dimensional aggregation kernels but using shorter and shorter time constants $1/(cN_0)$ of 5 yr, 1.5 yr, 0.5 yr and 0.05 yr. We run the computations starting at time $t = 0$ with the initial ^{26}Al content controlling the heat production H_0, until the largest planetesimal reaches a size of order 10^{20}-10^{21} kg. The average mass, the average temperature of the planetesimals (the mass averaged temperature of all the planetesimals of the swarm $\sum_{ij} N_{ij}\varepsilon_{ij}/(M_0C)$) and the temperature of the hottest planetesimal of the swarm can be readily extracted from the calculations (see Fig. 6). Notice that what we report as maximum temperature is the average temperature of the hottest planetesimal; the "maximum maximorum" temperature, i.e., the maximum temperature in the hottest planetesimal, assuming a parabolic profile should be $5/2$ larger. The average temperature (Fig. 6a) is the smooth function. The maximum temperature (Fig. 6b) is that of the bin with largest temperature that is populated. The various average planetesimal masses would be superposed if expressed as a function of the dimensionless time. The maximum planetesimal mass (not shown in Figure 6), for the chosen kernel, is ≈3000 times larger than the average mass.

In all cases, planetesimals have a negligible temperature until they reach a significant average

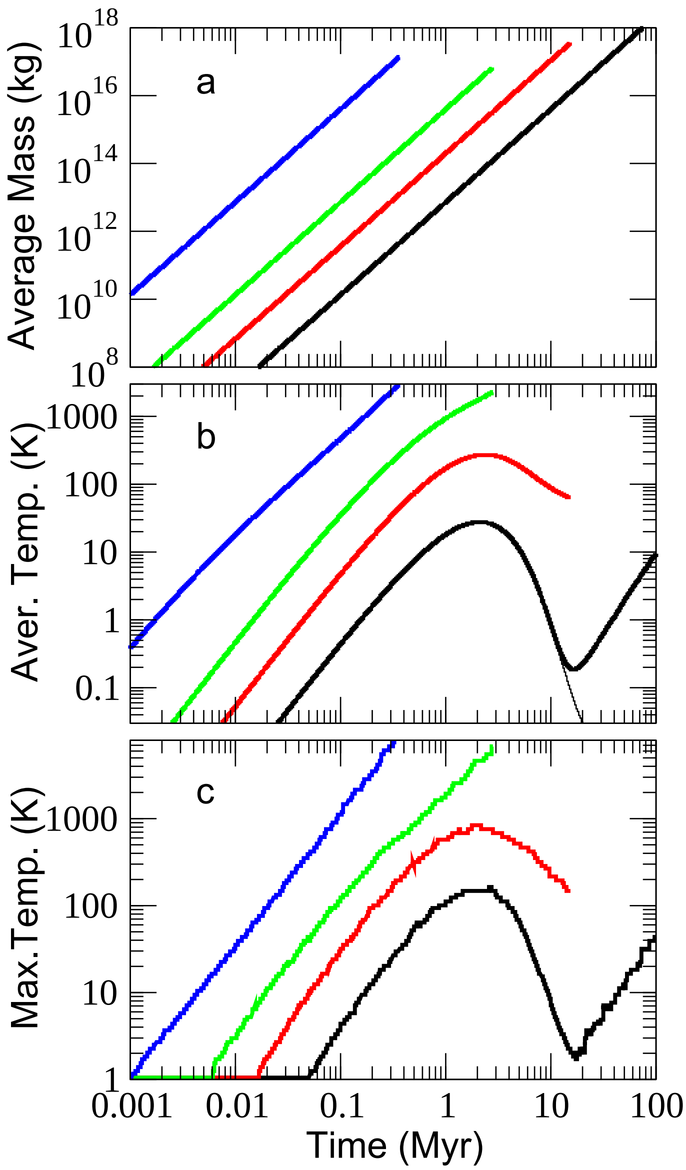

Figure 6: Evolution of mass and temperature for a planetesimal swarm heated by ^{26}Al and impact dissipation. Panel a: average planetesimal mass as a function of time. The maximum planetesimal in each situation is 3000 times more massive than the average planetesimal mass. Panel b: average temperature of the swarm of planetesimals as a function of time. The black and red dashed lines correspond to cases where gravitational heating is neglected. Panel c: average temperature of the hottest planetesimal. The aggregation kernels are $\Lambda = c(m, m')^{2/3}$ with $1/(cN_0)$ equal to 5, 1.5, 0.5 and 0.05 yr, for the black, red, green blue lines, respectively.

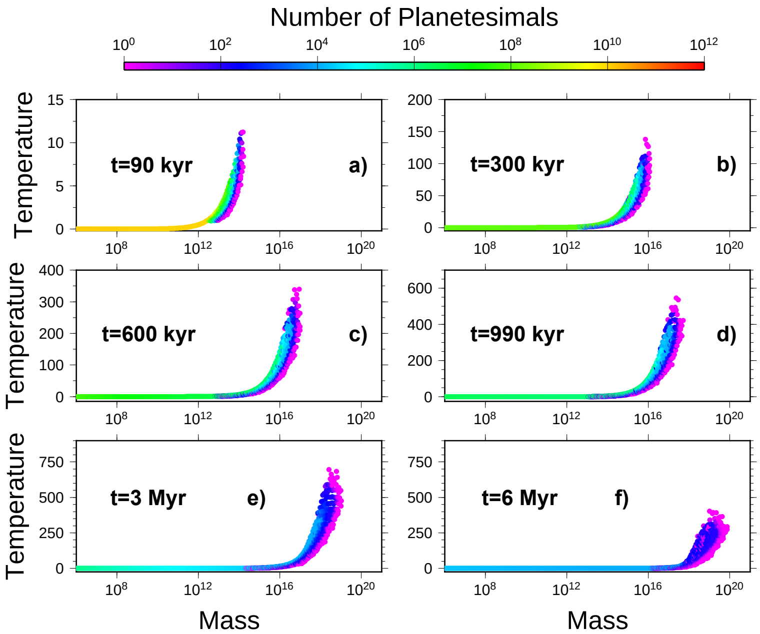

Figure 7: Joint mass-temperature distribution of planetesimals at different times, when the rate of merging is $\Lambda(m, m') = (m + m')^{2/3}$. The simulation starts with $N_0 = 10^{24}$ identical planetesimals and a time constant $1/(cN_0)$=1.5 yr. Note the change of temperature scale in the different panels. After 3 Myr, the cooling of the swarm is clearly visible. The average mass and temperature evolution of this swarm are depicted with red lines in Figure 6.

size (average mass $\approx 10^{11}$ kg, or radius $\approx$ 180 m; maximum mass $\approx 3 \times 10^{14}$ kg, or maximum radius 2.5 km). Radiogenic heating becomes inefficient after a couple of radioactive decay times τ. The maximum temperature reached in a swarm (Fig. 6c) is significantly larger than the average temperature in the case of slow accretion (a factor $\approx$ 6, compare the black lines of Figures 6 b and c) but only 3 times as large for a fast case (Fig. 6, b and c, blue lines). The impact heating remains rather inefficient until the average mass is $\approx 10^{18}$ kg and the largest mass $\approx 3 \times 10^{21}$ kg (the thin black line in Fig. 6 panel b, shows a case without impact heating). This is in agreement with (18) which, for these masses, predicts thermal contributions of 0.22 K and 45 K.

Figures 7 and 8 depict the distribution of temperatures and sizes of the planetesimal swarms at different times for the cases reported with the red and blue lines in Figure 6. Each color dot represents the number of planetesimals in a bin of given mass and temperature. In a slow-accretion scenario (Fig. 7, with $1/(cN_0)$ = 1.5 yr), the ^{26}Al is exhausted before the impact heating becomes significant, and the planetesimals should not melt before a second phase of temperature increase related to impact heating. In a fast-accretion scenario (Fig. 8, with $1/(cN_0)$ = 0.05 yr), radiogenic and collisional heating act simultaneously. In all cases, only the distribution of planetesimals in the mass range 10^{16}-10^{17} kg show significant dispersion of temperature.

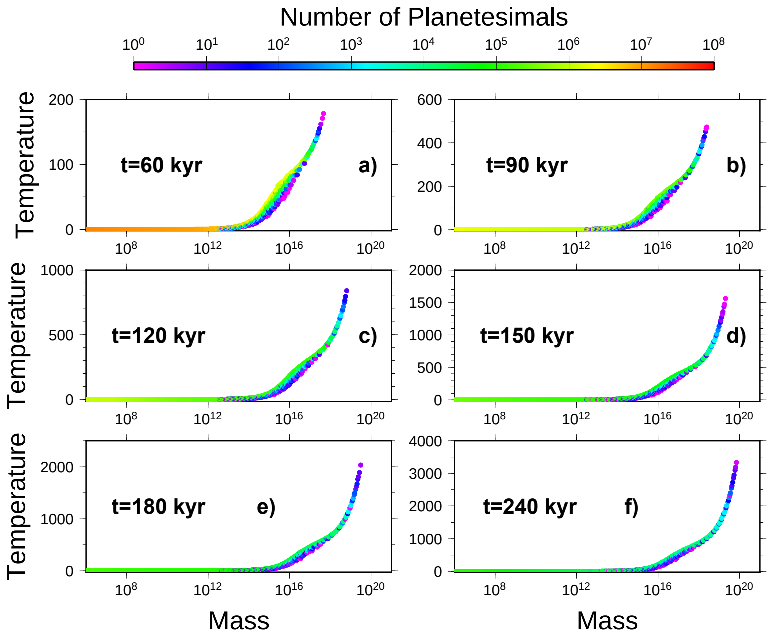

Figure 8: Same as Figure 7 but with a faster rate of aggregation ($1/(cN_0)$=0.05 yr).

5.3. Kernels with gravitational attraction

To simulate the runaway formation of planetesimals in which gravitational self attraction becomes important, we performed further simulations with the aggregation kernel

$$\Lambda(m, m') = c\left((m + m')^{2/3} + \frac{(m + m')^{4/3}}{(2\mu)^{2/3}}\right). \tag{42}$$

This kernel accounts for the enhanced cross sections of the planetesimals when their masses are larger than μ. We choose $\mu = 3 \times 10^{16}$ kg so that the escape velocity from a planetesimal of mass μ is comparable to the relative dust grain velocity in the nebula. The evolution of the mass distribution (Fig. 9) shows that until planetesimals become heavier than $\approx 10^{16}$ kg, their the evolution is the same as for a purely collisional kernel $\Lambda(m, m') \propto (m + m')^{2/3}$ (see Fig. 5). For heavier planetesimals, the evolution accelerates (in the first phase, the black, red, green and blue distributions correspond to times successively multiplied by 3, in the second phase the times between purple and cyan is only multiplied by 1.1), the distribution widens, the number of large planetesimals per bin becomes small and stochastic, and gaps appear in the distribution. A runaway planetesimal is formed when critical masses of about 10^{21} kg are present.

The joint mass and temperature evolutions for the composite kernel (42) (Fig. 10) can be compared with that without gravitational attraction (Fig. 6). Although the first phase of evolution for the two kernels is similar, the second phase, when gravitational attraction becomes efficient, leads to very fast accretion and runaway embryo growth. The resulting embryo grows in a few 10 kyr by capturing most of the other planetesimals and its temperature jumps very rapidly according to the estimate given by (18), i.e., approximately 2000 K. Depending on when the

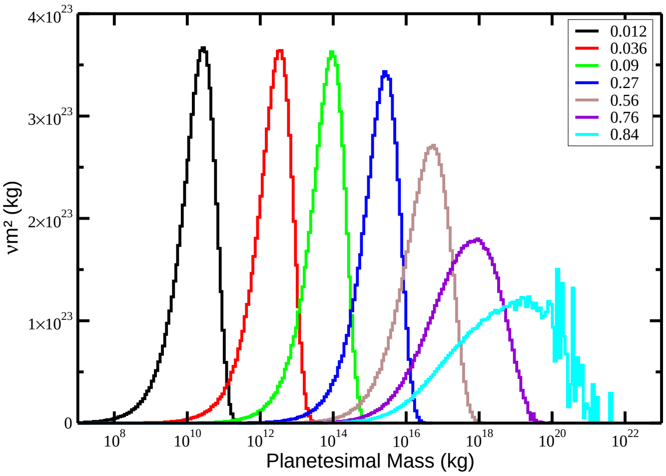

Figure 9: Mass distributions multiplied by m^2 plotted as a function of planetesimal masses for different dimensionless times (these times divided by 10^6 are indicated). The aggregation kernel is $\propto (m + m')^{2/3}$ until the masses are $\approx 3 \times 10^{16}$ (same as in Figure 5), then switches to $\propto (m + m')^{4/3}$. In this second phase, a runaway planetesimal is formed. Near the critical time of runaway (cyan), the distribution becomes discontinuous for large planetesimals and the low number of planetesimals in each mass bin makes the statistical character of the accretion conspicuous.

runaway coagulation starts, the final temperature of the embryo ranges between 2000 and 4000 K. An excessively slow aggregation rate allows the radioactive heat to be lost (Fig. 10, black curve) and the final temperature is around 2000 K. Very fast aggregation does not leave sufficient time for the radiogenic heat to accumulate before the formation of a planet, which therefore only heats up later. The maximum temperature, which is significantly larger than the average temperature (by a factor varying from 3 to 6), approaches the average temperature when most of the mass of the initial swarm is contained in the runaway embryo.

The distribution of temperatures and sizes of the planetesimal swarms at different times using the kernel (42) can also be inferred (Fig. 11). For less massive planetesimals (i.e., for which the kernel terms that go as $m^{2/3}$ are still significant), the evolution is identical to that of the collisional kernels, as expected (Fig. 7). By 900 kyr (Fig. 11a), some planetesimals with masses larger than $\mu = 3 \times 10^{16}$ kg start to attract the smaller planetesimals and grow faster, with a temperature close to the average of that of the largest planetesimals (Fig. 11c). Approximately 200 kyr later, a planetary embryo leaves the distribution (Fig. 11d) and concentrates most of the mass of the swarm (Fig. 11e). The cold and low masses remaining in the swarm are rapidly removed (Fig. 11f).

6. Discussion

We can summarize the findings of our model by considering three different accretion cases, in particular, fast accretion (wherein a planet embryo appears in 40 kyr), intermediate accretion (the embryo forms in 400 kyr) and slow accretion (the embryo appears in 4 Myr); see Fig. 12a,

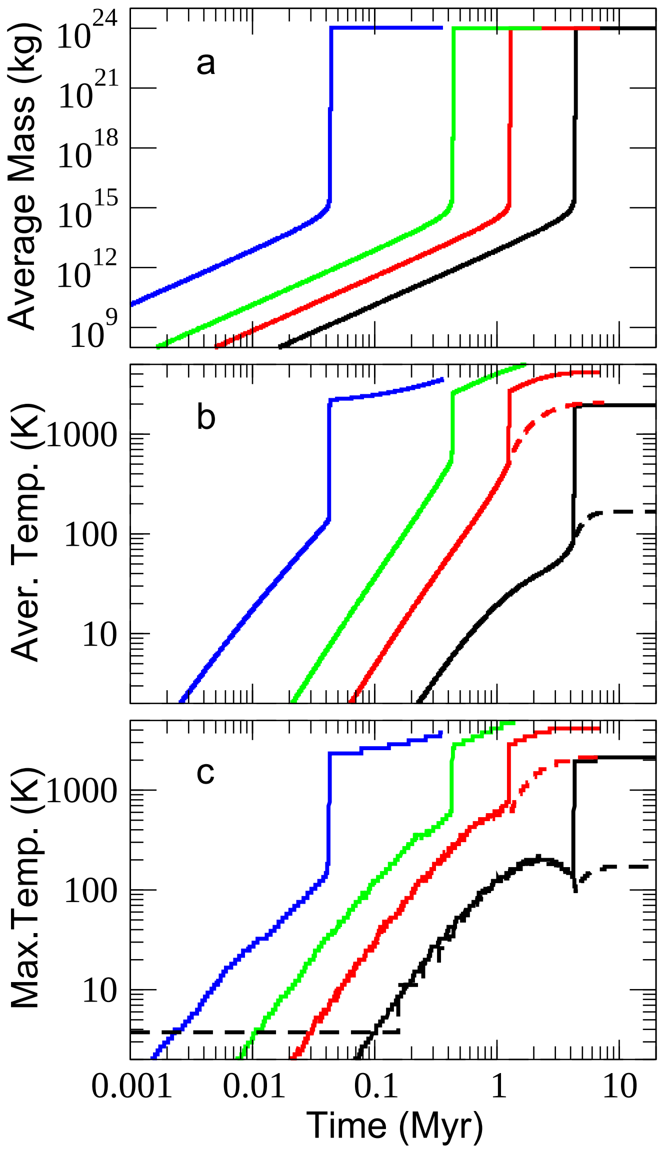

Figure 10: Evolution of mass and temperature for a planetesimal swarm heated by ^{26}Al and impact dissipation. Unlike the calculations shown in Figure 6, the aggregation kernel now accounts for the gravitational attraction between planetesimals, which leads to a runaway embryo growth. Panel a: average planetesimal mass as a function of time. Panel b: average temperature of the swarm as a function of time. The black and red dashed lines correspond to cases where gravitational heating is neglected. Panel c: temperature of the hottest planetesimal. The aggregation kernel is discussed in the text and we use $1/(cN_0)$ equal to 5, 1.5, 0.5 and 0.05 years, for the black, red, green blue lines, respectively.

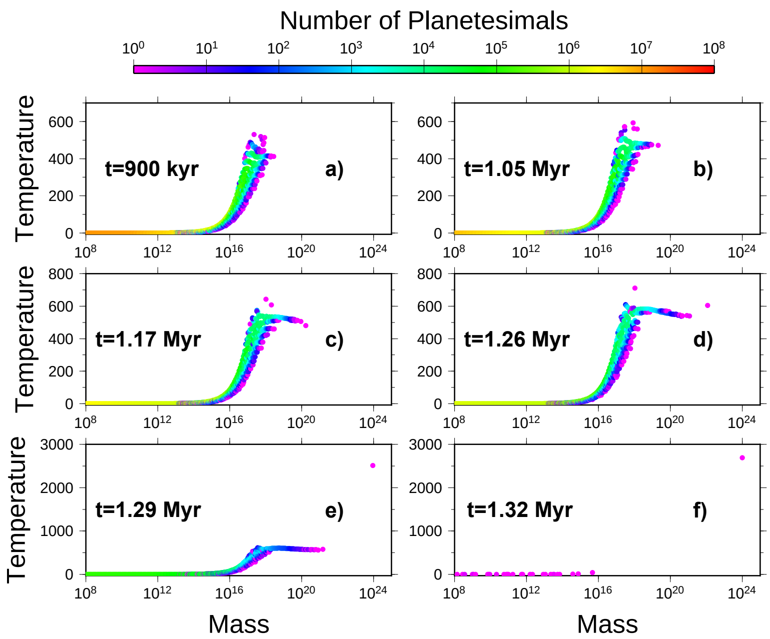

Figure 11: Mass and temperature distribution of a swarm of gravitationally self attracting planetesimals. The average mass and temperature evolution of this swarm are depicted with red lines in Figure 10 ($1/(cN_0) = 1.5$ yr). The panels are focussed on time close to the start of the embryo runaway; before $t = 900$ kyr, the swarm has a very similar evolution as in Figure 7. After this time, the largest planetesimals start to attract each other and to attract the smaller planetesimals. Rapidly growing embryo(s) are formed (c and d) and in a few 10 kyr; a planet containing most of the mass of the swarm is formed (e), leaving only a depleted swarm of cold and small planetesimals (f).

where blue, green and black curves represent fast, intermediate and slow accretion, respectively. The expression (40) that neglects diffusion and impact heating (orange curve) is sometimes used as a estimate for planetesimal temperature. It is however off by orders of magnitude for the case of slow accretion (Fig. 10 c, black curves) since the heat production has sufficient time to diffuse through the planetesimals and radiate away. Even in the case of a fast accretion, in which the thermal blanketing of rapidly added mass helps retain heat in the growing planetesimal, the maximum temperatures are 2-4 times lower than the estimate of equation (40). The average temperatures are themselves 2-10 times smaller that the maximum temperature, since most of the planetesimals are smaller and colder than the largest ones. For two faster-growth scenarios, the influence of radiogenic heating before runaway growth ensues is moderate, and thus leads to temperature increases of a couple of hundred degrees. For the fastest accretion case, ^{26}Al decay is active during growth of the embryo and thus drives a significant increase in temperature. In contrast, ^{26}Al becomes extinct during the slowest accretion scenario, and the embryo undergoes cooling (see Fig. 10). In the case of intermediate accretion, where an embryo is formed after 400 kyr, the planet reaches high enough temperatures for partial melting before runaway embryo growth.

The time and the mass of the largest planetesimal are directly related to each other for a given aggregation kernel, thus we can consider the embryo temperatures as a function of maximum planetesimal mass (Fig. 12b). We can then compare the maximum swarm temperatures to the estimates for steady state temperature with no impact heating (41) (Fig. 12b brown line) and with impact heating without ^{26}Al radioactivity and diffusion (18) (Fig. 12b purple line). The maximum swarm temperatures are in between these two estimates. Small planetesimals are colder than the no-impact heating estimate, because the quantity of ^{26}Al decreases with time and their temperatures are diluted by the accretion of smaller and colder objects. When embryo masses exceed $\approx 10^{21}$ kg, their temperature increase as they accumulate more mass, as expected for gravitational or impact heating.

Overall, the role of intense, short-lived radiogenic heating *before* the formation of solid planets is at most moderate. Either the objects are too small to conserve radiogenic heat, or they accrete too rapidly with respect to the ^{26}Al decay half-life. In the rapid-accretion case, the initial burst of radioactivity eventually plays an important role, but only after the planets are mostly formed. For example, we consider cases for the evolution of dwarf-planet sized bodies that remain isolated after slow (i.e. after 4 Myr), intermediate (400 kyr) and fast (40 kyr) accretion scenarios (Fig.13). For each accretion scenario, we consider final dwarf-planets that are either Vesta-size (3×10^{20} kg, Ghosh & McSween, 1998) or smaller (i.e. 10^{18} kg and 10^{16} kg). Following equation (14) (where m remains constant), the temperature evolves but melting can never happen in the slow accretion scenario: a Vesta size object must have been formed in less than 2 Myr to melt (i.e., to reach 900 K). A smaller object of 10^{18} kg or radius of 38 km (Fig. 13 blue curves) only melts if formed in less than 1 Myr. An even smaller object of 10^{16} kg or radius or 8 km (Fig. 13, green curves) can never reach a high enough temperature to melt, no matter when it is formed. However, note that we only consider here the very first planetesimals that reach a given dwarf-planet size; later in the accretion process other planetesimals with the same mass are formed. These subsequent planetesimals are generally colder because they remained small for a longer period during which thermal diffusion was therefore more efficient; moreover, they acquired much of the mass later, when radiogenic heating had diminished. However, the heaviest planetesimals are not necessarily always the hottest (Fig. 7 or 11). The distribution of maximum temperatures for planetesimals of a given size could be derived from our formalism, but this exercise is left for future work.

7. Conclusion

With our relatively simple accretion model, we have shown that the temperature distribution of planetesimals during their formation is feasible with a limited number of assumptions. Our approach is therefore significantly different to previous ones that only discuss the thermal evolution of a single accreting body assumed to be typical of a planetesimal swarm (e.g., Senshu et al., 2002; Yoshino et al., 2003; Merk & Prialnik, 2003; Walter & Tronnes, 2004; Merk & Prialnik, 2006; Sramek et al., 2012). For the sake of clarity, we purposely did not include various complexities that could easily be taken into account. For example, the model could consider the phenomenon of fragmentation during impact rather than assuming perfect coalescence (Wetherill & Stewart, 1993; Kobayashi et al., 2010). Further effects could be included as well, such as the temperature in the accretion disk, other radiogenic heat sources such as ^{60}Fe (Quitte et al., 2011), and more realistic heat deposition (during impact), transport (via convection) as well as the buffering effect of latent heat. All these possible improvements would not significantly change our numerical code or its execution time.

Our model suggests that melting of asteroids or minor planets (say masses $\approx 10^{20}$ kg) occurs only for those that are formed in less than 1-2 Myr. Most planetesimals of a given mass are, however, significantly colder than the leading planetesimal that has reached this mass, so that the leading planetesimal of mass 10^{20} kg has probably reached that size in less than a few 100 kyr (see Fig. 13). The melting of objects lighter than $\approx 10^{17}$ kg appears to be unlikely if not impossible. The temperature distribution that can be derived from our model can be compared with observations of meteorites, asteroids and dwarf planets. However, such a comparison must take into account the observational bias due to the fact that objects that have been molten (e.g. iron meteorites) have probably a higher survival rate. The fragmentation of minor planets very early during the accretion may also have replenished the disk with objects of small mass but that went through high temperature conditions. At any rate, out study shows that instead of focussing on the specific thermal history of a given object we can perform a statistical analysis of the conditions that prevailed in a planetesimal swarm. For the same final masses, different dwarf planets or different meteorites may have undergone very different thermal histories.

Acknowledgments

This work is supported by the Pallas program (ANR-14-CE33-0006-03).

Appendix A. General conservation laws

For any quantity $x(m, \varepsilon, t)$ specific to each planetesimal, the total quantity for the ensemble of planetesimals is

$$X = \iint x\mathcal{W}\,\mathrm{d}m\mathrm{d}\varepsilon. \tag{A.1}$$

If $x \equiv 1$, m or ε, then X is the total number N, the total mass M or the total energy E of all planetesimals, respectively. Because the integration limits of (A.1) are from 0 to ∞, the rate of change of X is simply

$$\frac{\mathrm{d}X}{\mathrm{d}t} = \iint \frac{\partial x\mathcal{W}}{\partial t}\,\mathrm{d}m\mathrm{d}\varepsilon = \iint \left(x\frac{\partial \mathcal{W}}{\partial t} + \mathcal{W}\frac{\partial x}{\partial t} \right) \mathrm{d}m\mathrm{d}\varepsilon \tag{A.2}$$

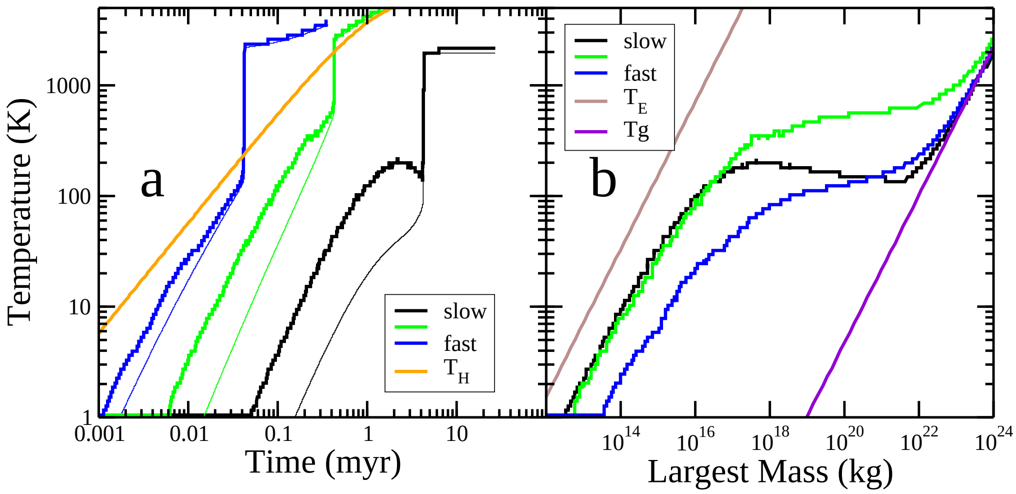

Figure 12: Panel a: Average temperature (thin) and maximum temperature (thick) in the planetesimal swarm as a function of time. The slow (black, $1/(cN_0) = 5$ yr), intermediate (green, $1/(cN_0) = 0.5$ yr), and fast (blue, $1/(cN_0) = 0.05$ yr) accretion scenarios are the same as those of Figure 10. The orange line corresponds to equation (40) which neglects heat diffusion and impact heating. Panel b: Maximum temperature in the planetesimal swarm, as in Panel a, but plotted as a function of the mass of the largest planetesimal at a given time. The green and purple lines correspond to the equation (41) of diffusive thermal equilibrium in the absence of impact heating, and (18) of pure impact heating.

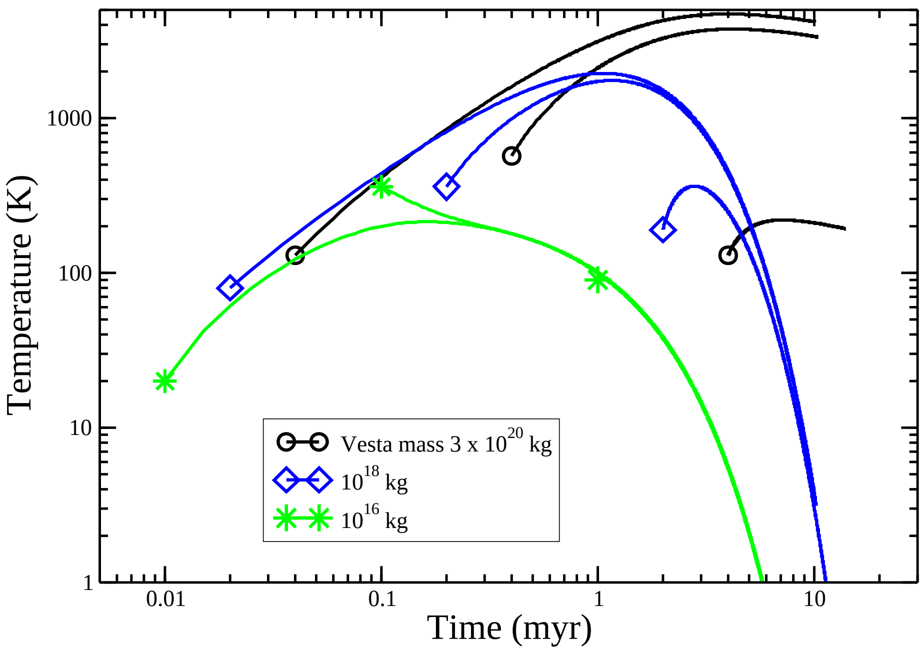

Figure 13: Evolution of the temperature of planetesimals that would have remained isolated after their formation (with Vesta mass, black curve; with a mass of 10^{18} kg, blue curve; and with a mass of 10^{16} kg, green curve). Each of these planetesimals were formed in either the slow ($1/(cN_0)$ = 5 yr), intermediate ($1/(cN_0)$ = 0.5 yr), or fast ($1/(cN_0)$ = 0.05 yr) accretion scenarios.

and according to (6),

$$\frac{\mathrm{d}X}{\mathrm{d}t} = \iint \left(x\Theta - x\frac{\partial \dot{\varepsilon}\mathcal{W}}{\partial \varepsilon} + \mathcal{W}\frac{\partial x}{\partial t} \right) \mathrm{d}m\mathrm{d}\varepsilon \tag{A.3}$$

The second term in the integral can be integrated by parts (i.e., $x\mathrm{d}(\dot{\varepsilon}\mathcal{W}) = \mathrm{d}(x\dot{\varepsilon}\mathcal{W}) - \dot{\varepsilon}\mathcal{W}\mathrm{d}x$), and the integral of $\mathrm{d}(x\dot{\varepsilon}\mathcal{W})$ cancels, leading to

$$\frac{\mathrm{d}X}{\mathrm{d}t} = \iint \left(x\Theta + \mathcal{W}\left[\frac{\partial x}{\partial t} + \dot{\varepsilon}\frac{\partial x}{\partial \varepsilon} \right] \right) \mathrm{d}m\mathrm{d}\varepsilon \tag{A.4}$$

The term within the square brackets is the total variation of x so that

$$\frac{\mathrm{d}X}{\mathrm{d}t} = \iint \left(x\Theta + \mathcal{W}\frac{\mathrm{d}x}{\mathrm{d}t} \right) \mathrm{d}m\mathrm{d}\varepsilon \tag{A.5}$$

This expression can be used to compute the rate of change of the total number, the total mass and the total energy of the planetesimal swarm. The total number of planetesimals N (using $x = 1$ and $\mathrm{d}x/\mathrm{d}t = 0$ in (A.5)) varies as

$$\frac{\mathrm{d}N}{\mathrm{d}t} = \iint \Theta \, \mathrm{d}m\mathrm{d}\varepsilon = \int \Gamma \, \mathrm{d}m = -\frac{1}{2}\iint \widetilde{R}(m', m") \, \mathrm{d}m'\mathrm{d}m" \leq 0 \tag{A.6}$$

(since $\int \widetilde{D} \, \mathrm{d}m = \int (\delta(m - m' - m") - \delta(m - m') - \delta(m - m")) \, \mathrm{d}m = -1$). The total number of planetesimals therefore decreases as $\widetilde{R}(m', m") \geq 0$. In the case $\widetilde{R}(m', m") = 1$, one has simply $\mathrm{d}N/\mathrm{d}t = -cN^2$, i.e., the average mass of planetesimals, M/N increases linearly with time.

The total mass of planetesimals, M is conserved (using $x = m$ in (A.5), and given that there is no continuous mass exchange $\dot{m} = 0$)

$$\frac{\mathrm{d}M}{\mathrm{d}t} = \iint m\Theta \, \mathrm{d}m\mathrm{d}\varepsilon = \int m\Gamma \, \mathrm{d}m = 0 \tag{A.7}$$

since $\int m\widetilde{D} \, \mathrm{d}m = \int m[\delta(m - m' - m") - \delta(m - m') - \delta(m - m")] \, \mathrm{d}m = (m' + m") - m' - m" = 0$.

If $x \equiv \varepsilon$, X is the total energy of planetesimals E, which evolves according to

$$\frac{\mathrm{d}E}{\mathrm{d}t} = \iint (\varepsilon\Theta + \mathcal{W}\frac{\mathrm{d}\varepsilon}{\mathrm{d}t}) \, \mathrm{d}m\mathrm{d}\varepsilon \neq 0 \tag{A.8}$$

The integral of $\varepsilon\Theta$ can be computed as $\int \varepsilon D \, \mathrm{d}m\mathrm{d}\varepsilon = \int \varepsilon[\delta(\varepsilon - \varepsilon' - \varepsilon" - \Delta\varepsilon) - \delta(\varepsilon - \varepsilon') - \delta(\varepsilon - \varepsilon")] \, \mathrm{d}\varepsilon = (\varepsilon' + \varepsilon" + \Delta\varepsilon) - \varepsilon' - \varepsilon" = \Delta\varepsilon$. Therefore using (14) and (17), the total energy evolution becomes

$$\begin{aligned} \frac{dE}{dt} =& MH_0 \exp(-t/\tau) \\ &+ G\left(\frac{4\pi\rho}{3}\right)^{1/3} \iint \frac{m'm"}{m'^{1/3} + m"^{1/3}} \Lambda(m', m")\mathcal{V}(m')\mathcal{V}(m")\mathrm{d}m'\mathrm{d}m" \\ &- 15\kappa\left(\frac{4\pi\rho}{3}\right)^{2/3} \iint \mathcal{W}(m, \varepsilon)\varepsilon m^{-2/3} \, \mathrm{d}m\mathrm{d}\varepsilon \neq 0 \end{aligned} \tag{A.9}$$

where the radiogenic heating, gravitational heating and heat loss controlled by diffusion are evident in the first, second and third terms on the right side (A.9), respectively. Therefore, the total number of planetesimals is decreasing, their total mass is conserved and their total energy can increased by radiogenic and/or impact heating, or decreased by diffusive heat loss.

Ackleh, A. S. & Fitzpatrick, B. G., 1997. Modeling aggregation and growth processes in an algal population model: Analysis and computations, *J. Math. Biol.*, **35**, 480–502.

Agee, C., Li, J., Shannon, M., & Circone, S., 1995. Pressure-Temperature Phase-Diagram For The Allende Meteorite, *J. Geophys. Res.-Solid Earth*, **100**(B9), 17725–17740.

Bercovici, D. & Ricard, Y., 2012. Mechanisms for the generation of plate tectonics by two-phase grain damage and pinning, *Phys. Earth Planet. Int.*, **202-203**, 27–55.

Bercovici, D. & Ricard, Y., 2013. Generation of plate tectonics with two-phase grain- damage and pinning: Sourcesink model and toroidal flow, *Earth Planet. Sci. Lett.*, **365**, 275–288.

Bercovici, D. & Ricard, Y., 2014. Plate tectonics, damage and inheritance, *Nature*, **508**, 513–516.

Birch, F., 1965. Energetics of core formation, *J. Geophys. Res.*, **70**(24), 6217–&.

Collet, J.-F., 2004. Some modelling issues in the theory of fragmentation-coagulation systems, *Comm. Math. Sci.*, **1**, 35–54.

Collet, J. F. & Goudon, T., 2000. On solutions of the Lifshitz-Slyozov model, *Nonlinearity*, **13**, 1239–1262.

Flasar, F. & Birch, F., 1973. Energetics of core formation (vol 70, pg 6217, 1965), *J. Geophys. Res.*, **78**(26), 6101–6103.

Gelbard, F. & Seinfeld, J., 1979. General dynamic equation for aerosols - Theory and application to aerosol formation and growth, *J. Colloid Interface Sci.*, **68**(2), 363–382.

Ghosh, A. & McSween, H., 1998. A thermal model for the differentiation of Asteroid 4 Vesta, based on radiogenic heating, *Icarus*, **134**(2), 187–206.

Hillert, M., 1965. On the theory of normal and abnormal grain growth, *Acta Metallurgica*, **13**, 227–238.

Hirschmann, M. M., 2000. Mantle solidus: Experimental constraints and the effects of peridotite composition, *Geochim. Geophys. Geosys.*, **1**.

Inaba, S., Tanaka, H., Ohtsuki, K., & Nakazawa, K., 1999. High-accuracy statistical simulation of planetary accretion: I. Test of the accuracy by comparison with the solution to the stochastic coagulation equation, *Earth Planets Space*, **51**(3), 205–217.

Inaba, S., Tanaka, H., Nakazawa, K., Wetherill, G., & Kokubo, E., 2001. High-accuracy statistical simulation of planetary accretion: II. Comparison with N-body simulation, *Icarus*, **149**(1), 235–250.

Izidoro, A., Haghighipour, N., Winter, O. C., & Tsuchida, M., 2014. Terrestrial planet formation in a protoplanetary disk with a local mass depletion: a successful scenario for the formation of mars, *Astrophys. J.*, **782**(1).

Kenyon, S. & Luu, J., 1998. Accretion in the early Kuiper Belt. I. Coagulation and velocity evolution, *Astron. J.*, **115**(5), 2136–2160.

Kobayashi, H., Tanaka, H., Krivov, A. V., & Inaba, S., 2010. Planetary growth with collisional fragmentation and gas drag, *Icarus*, **209**(2), 836–847.

Kortenkamp, S. J., Kokubo, E., & Weidenschilling, S., 2000. Formation of planetary embryos, in *Origin of the Earth and Moon*, edited by R. M. Canup & K. Righter, pp. 85–100, The University of Arizona Press, Tucson.

Lambrechts, M. & Johansen, A., 2012. Rapid growth of gas-giant cores by pebble accretion, *Astron. & Astrophys.*, **544**.

Lee, T., Papanastassiou, D., & Wasserburg, G., 1976. Demonstration of mg-26 excess in allende and evidence for al-26, *Geophys. Res. Let.*, **3**(2), 109–112.

Levison, H. F., Kretke, K. A., & Duncan, M. J., 2015. Growing the gas-giant planets by the gradual accumulation of pebbles, *NATURE*, **524**(7565), 322+.

Leyvraz, F. O., 2005. Rigorous results in the scaling theory of irreversible aggregation kinetics, *J. Nonlinear Math. Phys.*, **12**, 449–465.

Lifshitz, I. M. & Slyozov, V. V., 1961. The kinetics of precipitation from supersaturated solid solutions, *J. Phys. Chem. Solids*, **19**, 35–50.

Merk, R. & Prialnik, D., 2003. Early thermal and structural evolution of small bodies in the trans-Neptunian zone, *Earth Moon Planets*, **92**(1-4), 359–374.

Merk, R. & Prialnik, D., 2006. Combined modeling of thermal evolution and accretion of trans-neptunian objects - Occurrence of high temperatures and liquid water, *Icarus*, **183**(2), 283–295.

Merk, R., Breuer, D., & Spohn, T., 2002. ^{26}Al-induced radioactive melting of asteroids considering accretion, *Icarus*, **159**, 183–191.

Monteux, J., Ricard, Y., Coltice, N., Dubuffet, F., & Ulvrova, M., 2009. A model of metal-silicate separation on growing planets, *Earth Planet. Sci. Lett.*.

Morbidelli, A., Bottke, W. F., Nesvorny, D., & Levison, H. F., 2009. Asteroids were born big, *Icarus*, **204**(2), 558–573.

Morfill, G. E. & Wood, J. A., 1989. Protoplanetary Accretion Disk Models - the Effects of Several Meteoritic, Astronomical, tnd Physical Constraints, *Icarus*, **82**(2), 225–243.

Nakagawa, Y., Sekiya, M., & Hayashi, C., 1986. Settling And Growth Of Dust Particles In A Laminar Phase Of A Low-Mass Solar Nebula, *Icarus*, **67**(3), 375–390.

Neelamegham, S., Munn, L. L., & Zygourakis, K., 1997. Model for the kinetics of homotypic cellular aggregation under static conditions, *Biophys. J.*, **72**, 51–64.

Ohtsuki, K., Nakagawa, Y., & Nakazawa, K., 1990. Artificial acceleration in accumulation due to coarse mass-coordinate divisions in numerical-simulation, *Icarus*, **83**(1), 205–215.

O'Keefe, J. D. & Ahrens, T. J., 1977. Impact-induced energy partitioning, melting, and vaporization on terrestrial planets, in *Lunar and Planetary Science Conference Proceedings*, edited by R. B. Merril, vol. 8, pp. 3357–3374.

Pierazzo, E. & Melosh, H., 2000. Understanding oblique impacts from experiments, observations, and modeling, *Ann. Rev. Earth Planet. Sci.*, **28**, 141–167.

Pilinis, C., 1990. Derivation and numerical-solution of the species mass-distribution equations for multicomponent particulate systems, *Atmos. Environ.*, **24**(7), 1923–1928.

Quitte, G., Latkoczy, C., Schoenbaechler, M., Halliday, A. N., & Guenther, D., 2011. Fe-60-Ni-60 systematics in the eucrite parent body: A case study of Bouvante and Juvinas, *Geochim. Cosmochim. Acta*, **75**(23), 7698–7706.

Randolph, A. D. & Larson, M. A., 1988. *Theory of particulate process: Analysis and techniques of continuous crystallization*, Academic Press.

Ricard, Y. & Bercovici, D., 2009. A continuum theory of grain size evolution and damage, *J. Geophys. Res.*, **114**.

Ricard, Y., Sramek, O., & Dubuffet, F., 2009. A multi-phase model of runaway core-mantle segregation in planetary embryos, *Earth Planet. Sci. Lett.*, **284**, 144–150.

Rozel, A., Ricard, Y., & Bercovici, D., 2011. A thermodynamically self-consistent damage equation for grain size evolution during dynamic recrystallization, *Geophys. J. Inter.*, **184**(2), 719–728.

Safronov, V., 1962. Particular case of solution to coagulation equation, *Dok. Akad. Nauk SSSR*, **147**(1), 64–&.

Senshu, H., Kuramoto, K., & Matsui, T., 2002. Thermal evolution of a growing Mars, *J. Geophys. Res.*, **107**(E12), 5118.

Solomon, S., 1979. Formation, History And Energetics Of Cores In The Terrestrial Planets, *Phys. Earth Planet. Int.*, **19**(SI), 168–182.

Spohn, T. & Schubert, G., 1982. Modes Of Mantle Convection And The Removal Of Heat From The Earths Interior, *J. Geophys. Res.*, **87**(NB6), 4682–4696.

Sramek, O., Milelli, L., Ricard, Y., & Labrosse, S., 2012. Thermal evolution and differentiation of planetesimals and planetary embryos, *Icarus*, **217**(1), 339–354.

Sramek, O., Ricard, Y., & Dubuffet, F., 2010. A multiphase model of core formation, *Geophys. J. Inter.*, **181**(1), 198–220.

Stewart, G. & Wetherill, G., 1988. Evolution of planetesimal velocities, *Icarus*, **74**(3), 542–553.

Stockmayer, W. H., 1943. Theory of molecular size distribution and gel formation in branched-chain polymers, *J. Chem. Phys.*, **11**, 45–55.

Tonks, W. B. & Melosh, H. J., 1993. Magma ocean formation due to giant impacts, *J. Geophys. Res.*, **98**(E3), 5319–5333.

Trubnikov, B., 1971. Solution to coagulation equations with bilinear coefficient of particule adhesion, *Dok. Akad. Nauk SSSR*, **196**(6), 1316–&.

von Smoluchowski, M., 1917. Experiments on a mathematical theory of kinetic coagulation of coloid solutions., *Z. Fur Physikalische Chemie–stochiometrie Und Verwandtschaftslehre*, **92**, 129–168.

Walsh, K. J., Morbidelli, A., Raymond, S. N., O'Brien, D. P., & Mandell, A. M., 2011. A low mass for Mars from Jupiter's early gas-driven migration, *NATURE*, **475**(7355), 206–209.

Walter, M. J. & Tronnes, R. G., 2004. Early Earth differentiation, *Earth Planet. Sci. Lett.*, **225**(3-4), 253–269.

Weidenschilling, S. J., 1988. Formation processes and time scales for meteorite parent bodies, in *Meteorites and the Early Solar System*, edited by Kerridge, J. F. and Metthews, S. W. , vol. 41 of **Univ. Arizona Press, Tucson.**, p. 348371.

Wetherill, G., 1990. Comparison of analytical and physical modeling of planetesimal accumulation, *Icarus*, **88**(2), 336–354.

Wetherill, G. & Stewart, G., 1989. accumulation of a swarm of small planetesimals, *Icarus*, **77**(2, 1), 330–357.

Wetherill, G. & Stewart, G., 1993. Formation Of Planetary Embryos - Effects Of Fragmentation, Low Relative Velocity, And Independent Variation Of Eccentricity And Inclination, *Icarus*, **106**(1), 190–209.

Wettlaufer, J. S., 2010. Accretion In Protoplanetary Disks By Collisional Fusion, *Astrophys. J.*, **719**(1), 540–549.

Whipple, F., 1964. History Of Solar System, *Proc. Nation. Acad. Sci. US Am.*, **52**(2), 565–&.

Yoshino, T., Walter, M. J., & Katsura, T., 2003. Core formation in planetesimals triggered by permeable flow, *Nature*, **422**, 154–157.

Youdin, A. N., 2010. From Grains To Planetesimals, in *Physics And Astrophysics Of Planetary Systems*, edited by Montmerle, T and Ehrenreich, D and Lagrange, AM, vol. 41 of **EAS Publications Series**, pp. 187–207.